Article:

Bos, F. orcid.org/0000-0002-6666-2395, Menna, C. orcid.org/0000-0001-9528-1324, Robens-Radermacher, A. orcid.org/0000-0001-9653-6085 et al. (12 more authors) (2025) Mechanical properties of 3D printed concrete: a RILEM TC 304-ADC interlaboratory study — approach and main results. Materials and Structures, 58 (5). 183. ISSN 1359-5997

https://doi.org/10.1617/s11527-025-02686-x

Materials and Structures (2025) 58:183
https://doi.org/10.1617/s11527-025-02686-x

RILEM TC REPORT

Mechanical properties of 3D printed concrete: a RILEM TC 304-ADC interlaboratory study — approach and main results

Freek Bos · Costantino Menna · Annika Robens-Radermacher · Rob Wolfs · Nicolas Roussel · Hélène Lombois-Burger · Bilal Baz · Daniel Weger · Behzad Nematollahi · Manu Santhanam · Yamei Zhang · Shantanu Bhattacherjee · Zijian Jia · Yu Chen · Viktor Mechtcherine

Received: 28 November 2024 / Accepted: 12 May 2025

Abstract To show compliance to structural engineering codes and implement quality control measures, it is critical to obtain reliable mechanical properties of the materials in question. For conventional cast and precast concrete, the experimental procedures and relationships between mechanical properties, the material composition, and the production methods are globally known, but for 3D concrete printing (3DCP), these relations have not yet been established. Previous studies have shown little consistency in results, and the underlying experimental methods have not been established broadly. There is an urgent need to address these issues as the application of 3DCP in practice projects is growing rapidly. Therefore, RILEM TC 304-ADC: *Assessment of Additively Manufactured Concrete Materials and Structures* has set up a large interlaboratory study into the mechanical properties of 3D printed concrete.

This paper has been prepared by representatives of participating laboratories and a writing group within the framework of RILEM TC 304-ADC 'Assessment of Additively Manufactured Concrete Materials and Structures' and further reviewed and approved by all members of the RILEM TC 304-ADC.

TC Chair Viktor Mechtcherine **TC Deputy chair** Freek Bos **TC Members** Rebecca Ammann, Arun Arunothayan, Daniel Auer, Bilal Baz, Shantanu Bhattacherjee, David Böhler, Richard Buswell, Laura Caneda Martinez, Jean-François Caron, Yu Chen, Maximilian Dahlenburg, Victor de Bono, Geert De Schutter, Laura Esposito, Claudia Eugenin, Liberato Ferrara, Niklas Freund, Lukas Gebhard, Lucija Hanžič, Ilhame Harbouz, C. Maximilian Hechtl, Muhammad Nura Isa, Egor Ivaniuk, Smrati Jain, Zijian Jia, Zhengwu Jiang, Jörg Jungwirth, Abdelhak Kaci, Emmanuel Keita, John Kolawole, Jacques Kruger, Cezary Kujath, Lucas Lima, Xingzi Liu, Hélène Lombois-Burger, Dirk Lowke, Inka Mai, Costantino Menna, Luiza Miranda, Renate Monte, Sandro Moro, Jean-Pierre Mostert, Shravan Muthukrishnan, Iván Navarrete, Tobias Neef, Behzad Nematollahi, Onur Ozturk, Nilufer Ozyurt, Said Rahal, Inken Jette Rasehorn, Atta Ur Rehman, Christiane Richter, Annika Robens-Radermacher, Josef Roupec, Nicolas Roussel, Aljoša Šajna, Manu Santhanam, Alise Sapata, Maris Sinka, Chalermwut Snguanyat, Mateja Štefančič, Katarina Šter, Kolluru Subramaniam, Markus Taubert, Jörg F. Unger, Jolien Van Der Putten, Kim Van Tittelboom, Gideon van Zijl, Jelle Versteege, Zhendi Wang, Timothy Wangler, Daniel Weger, Rob Wolfs, Yamei Zhang, Yi Zhang, Zengfeng Zhao.

F. Bos (✉)
Technical University of Munich, Munich, Germany
e-mail: freek.bos@tum.de

C. Menna
University of Naples Federico II, Naples, Italy

A. Robens-Radermacher
Bundesanstalt Für Materialforschung Und -Prüfung, Berlin, Germany

R. Wolfs
Eindhoven University of Technology, Eindhoven, The Netherlands

N. Roussel
Gustave Eiffel University, Paris, France

Published online: 24 June 2025

This paper presents key elements of the experimental approach detailed in the Study Plan and the supporting considerations. Furthermore, it reports on the response, consisting of 34 contributions from 30 laboratories, detailing global coverage, properties of the applied mixture designs and characteristics of the printing facilities that have been used. Subsequently, some fundamental results from compression, flexural, and E-modulus testing are presented and—considering cast specimens as a reference—discussed. On average, a reduction in strength was found in compression and E-modulus (all tested orientations). For flexure, on the other hand, an increase was found in two testing orientations, while a decrease was observed in the third orientation. Importantly, even though the applied experimental methods were found to be reasonably appropriate to obtain the required data, the differences found between individual contributions are significant and sometimes non-consistent, suggesting that testing on specific material-facility combinations is necessary to reliably determine the mechanical properties of objects produced from them. Furthermore, a theoretical framework needs to be developed to further explain the variations that were observed. Extensive analyses of all acquired data are out of the scope of this contribution, but presented in two associated papers, whereas a third presents the data management approach used to process the approximately 5,000 test results.

Keywords 3D printed concrete · 3DCP · Mechanical properties · Interlaboratory study

1 Introduction

Research and application of Digital Fabrication with Concrete (DFC) in the construction industry has enjoyed a rapid growth over the last decade [1]. DFC processes are characterized by a digital control over the design and manufacturing process [2]. A classification of the various DFC processes has been proposed by [3] and further elaborated by [4]. An extensive, in-depth discussion of DFC is provided by [5]. By far the most widely used DFC method, both in practice and academia, is *material deposition by extrusion*, also known as 3D concrete printing (3DCP). There is increasing interest within the industry to apply newly developed production and construction method in practice, mainly driven by cost savings and overall sustainability perspectives [6], as is showcased by a rapidly expanding body of built projects [7].

Amongst others, such projects need to meet requirements regarding structural performance as dictated by local construction regulations and structural codes. Code compliance is typically shown through calculations for which mechanical materials properties are required as input of the structural design, which are obtained through experimental testing. Subsequently, it must be verified that the structural elements that are produced and used in the construction actually meet the mechanical properties that were assumed in the structural calculations (net of safety factors). For the application of conventional cast or precast concrete, procedures to determine mechanical properties of the materials and verifications of the structural performance have been established, fine-tuned, and updated for decades (e.g., Eurocode 2 series [8], ACI 318 [9], *fib* Model Code [10], etc.). However, these procedures are not directly applicable to 3DCP without further consideration, because these novel fabrication processes differ considerably from cast/precast concrete in a number of important aspects. Besides the material composition (so far generally not actually concretes according to codified

H. Lombois-Burger · B. Baz
Holcim Innovation Center, Lyon, France

D. Weger
Ingenieurbüro Schiessl Gehlen Sodeikat GmbH, Munich, Germany

B. Nematollahi
University of Sheffield, Sheffield, UK

M. Santhanam
Indian Institute of Technology Madras, Chennai, India

Y. Zhang · Z. Jia
Southeast University, Nanjing, China

S. Bhattacherjee
Tvasta Manufacturing Pvt. Ltd., Bangalore, India

Y. Chen
Delft University of Technology, Delft, The Netherlands

V. Mechtcherine
TUD Dresden University of Technology, Dresden, Germany

definitions, but mortars – although we will use the term ‘concrete’ for reasons of simplicity) and issues related to typical geometrical thin-walled properties of printed objects (which will remain out of scope of in this paper), the diversity from normal concrete is mainly caused by the particularities of the digitally controlled additive fabrication process.

Besides the typical stacking of layers and the absence of formwork, it should be noted that 3DCP typically implies that a considerable number of process parameters can be set (nozzle velocities, material flow rate, pressures, layer offsets, output flows, layer thickness etc.). Furthermore, the applied facilities are defined by a number of fixed or semi-fixed characteristics (such as dimensional range of the automated movements, end effector etc. [11]) that may also influence the mechanical properties of the resulting object. Finally, interaction of the material, machinery and printed object with the ambient environment (temperature, relative humidity) will likely play a larger role than in cast concrete (generally following environmental conditioning set by standards), as for instance machine temperature can significantly influence material temperature and thereby structuration characteristics [12], while ambient conditions also affect the freshly deposited material [13].

It is widely recognized that a strong interaction between the printable material, process parameters and mechanical properties of the produced objects exists [14]. However, the relationships governing these interactions are not very well understood as many studies showed widely disparate quantitative results. To illustrate this and considering the direction nomenclature defined in [13] and illustrated in Figs. 12, 13, 14, 15, 16 and 17, the difference of flexural strength of u.w-orientation specimens compared to v.u-orientation is evaluated in studies by Le et al. [15], Nerella et al. [16], and Wolfs et al. [17]. The first found a difference of approximately −67%, while the second recorded reductions of around −50% and −20% for two different print materials. The latter, finally, only observed a change of around −10%.

The root of these differences remains unknown or confined to very specific materials/machinery studies, as well as to the nature of the weak interfaces/waiting time. A complicating factor to further study these issues is the lack of commonly accepted experimental methods to characterize the basic mechanical properties of printed materials in the hardened state (e.g., compression strength, flexural strength etc.). Most experimental studies on 3DCP use test methods that are based on existing mortar or concrete testing codes and guidelines. For the execution of the experiments themselves, this usually requires no or only minor adaptations. However, for the size, production and preparation of experimental specimens, this is different. Here, there is practically no commonly accepted methodology available, and each study develops its own methods based on the capabilities of the own printing facility and the academic engineering judgment of the respective authors. As a result, the outcomes are difficult to compare and general trends hard to identify. Newly emerging guidelines on the use of 3DCP provide little to no direction.

Meanwhile, in industrial practice, commercial entities have started to develop their own design, testing and approval guidelines to smoothen approval of using their methods in construction projects [18]. This underlines the importance of developing commonly accepted methods of determining mechanical properties and mechanical quality control of 3D printed concrete.

To facilitate an in-depth understanding of the mechanical properties of 3D printed concrete and develop common testing methods, the RILEM Technical Committee (TC) 304-ADC has initiated an interlaboratory study on the mechanical properties of 3D printed concrete (ILS-mech).

The study was prepared in 2022 by a preparation group consisting of the authors of the current paper. This resulted in a Study Plan that was approved by the TC on 29 November 2022, and subsequently published as an Open Access dataset [19]. The Study Plan provides a detailed description of the experimental procedures regarding specimen preparation, curing and testing that were maintained by the participating laboratories. It was developed based on an extensive inventory of the specifics in characterizing the mechanical properties of additively manufactured, cement-based materials presented by a group of authors from the same TC. The current paper reports on the study approach and underlying considerations, discusses the response and presents some main experimental results. This paper does not contain all details and outcomes therein but rather focuses on the major elements and motivations behind the chosen procedures as well as the practical issues and feedback that arose during the interlaboratory study. For further details on the preparation and execution of tests, the reader is kindly referred to the Study Plan.

Any laboratory represented in the TC and meeting the Study Plan requirements could participate in the study. The ILS-mech was performed in 2023 and yielded a sizeable set of data based on approximately 5,000 tested specimens. The data was collected using a preprepared spreadsheet template. The data processing and analysis method is presented in a separate publication [20], while in-depth analyses of the results for tensile properties and compressive properties are also the focus of two additional papers [21, 22]. The data has been assembled in a publicly accessible database for future use and analyses [23].

This paper is structured as follows. In Sect. 2, we outline the general considerations of the ILS-mech, including the objective, scope and methodology. Section 3 presents the experimental program, while Sect. 4 discusses the particularities of specimen preparation and the execution of the tests, including many considerations specific to testing of 3D printed concrete. The response of the ILS-mech is presented in Sect. 5, while some main results are shown and discussed in Sect. 6. Finally, in Sect. 7 we go into feedback and experiences regarding the experimental method, before presenting the conclusions in Sect. 8.

2 General considerations

2.1 Aim and objectives

The overall aim of the ILS-mech study was to better understand and quantitatively assess the relevance of the additive manufacturing process parameters as well as specimen extraction and handling methodology with respect to key mechanical properties of hardened print material. This knowledge is instrumental in developing future recommendations on material testing with respect to (1) determining properties needed for structural design (mainly compression and traction properties) and (2) effective quality control.

To address the aim, an extensive experimental work plan was developed. The experimental work plan was designed to answer the objectives of this study, which were to obtain quantitative data on:

- the difference between mechanical properties of cast and printed specimens,
- the variance in strength characteristics and modulus of elasticity for printed cementitious materials,
- the relationships between individual mechanical characteristics,
- the influence of orientation loading to layers and the effect of interfaces between layers in specimens,
- the specimen size effect (including the number of interfaces in a specimen),
- the influence of some key process variables typically associated with printing and curing.

Furthermore, we expected to obtain feedback from the participating laboratories on the feasibility and suitability of the proposed experimental methods. This would be useful for the formulation of recommendations for testing in the future.

2.2 Scope and methodology

The ILS-mech study concentrated on relatively simple mechanical tests, such as those used in codes for conventional concrete and mortar mechanical characterization, that were to be performed on locally produced specimens. It was expected that the interchangeability of mixture compositions on different printing facilities would be limited. Therefore, it was decided that each participating laboratory would select one or more materials to use and print the objects from which the specimens for mechanical testing were to be obtained. Hence, the study does not actually test materials or facilities, but rather material-facility combinations. It was recognized that this limits the comparability of the absolute results. However, it would allow a much wider group of laboratories to participate, and it was expected to effectively represent the reality in which many material-facility combinations are used.

The print materials themselves investigated in this interlaboratory study were cementitious in nature. Both one-component (K1) and multi-component (multi-K, e.g., K2, K3) systems, i.e. requiring the addition of a viscosity modifier or setting accelerator immediately before deposition, were allowed.

Table 1 Overview of experimental variables and values considered in the interlaboratory study

Variable	Value
Material characteristic to be obtained	• Compressive strength • Flexural strength • Splitting tensile strength • Uniaxial tensile strength • Modulus of elasticity (in compression)
Scale	• "Mortar", i.e. specimen dimensions in order of several centimeters • "Concrete", i.e. specimen dimensions in order of several tens of centimeters. Note that the terms "mortar" and "concrete" here only refer to the scale of the specimens, not to a variation in the material. All tests from a single laboratory contribution were performed with the same material. In the current paper, only mortar-scale results are discussed. Concrete-scale results are reported in [21, 22] 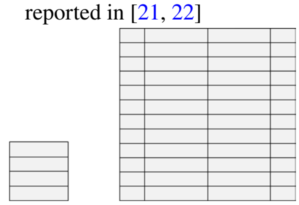
Specimen and load orientation	2–3 orientations, depending on the specific test
Mode of extraction	• Sawing • Core-drilling
Process parameter	• Default • Dev1 • Dev2

Alternative binders such as geopolymers or alkali-activated materials were out of the scope of this study. Specifically, the materials were not to contain structural fibers, as they require different experimental procedures to obtain the relevant mechanical properties (e.g., post-fracture).

The applied mixtures were required to be printable. However, since 'printable' is a relative requirement depending on the object design and printing facility/strategy and has not been quantitatively defined (although the underlying parameters that contribute to this ability have been studied), it was specified that the materials would have to be sufficiently 'buildable' to print the experimental objects as defined in the Study Plan.

Some requirements are also considered in terms of filament dimensions; for instance, in the mortar scale specimens, no more than 2 adjacent layers must be present when the interface is in the middle.

3 Experimental program

An extensive experimental program was designed, as summarized in Table 1. However, only a limited part of that was compulsory for all participating laboratories—most was optional.

For the experimental program, tests were proposed to determine five main print material characteristics in the hardened state: compressive strength, compressive modulus of elasticity, flexural strength and two types of tensile strength (splitting and uniaxial). These were considered the most relevant for structural engineering purposes. The inclusion of modulus of elasticity was considered particularly important as very little data on this property has previously been published.

Although they do not all apply equally to each test, four additional experimental variables were additionally suggested and included in the program: specimen-to-load orientation, scale, extraction mode, and process parameter.

The specimen-to-load orientation is the most obvious novel variable in comparison to traditional cast concrete. The printing process (specifically, the concrete filament additive deposition) introduces filament interfaces that generate anisotropy in the printed object [13]. Depending on the test type, 2 or 3 orientations were required for the specific mechanical property characterization. These orientations were defined in the Study Plan [19], based on the definitions according to [13].

It is known that the mechanical properties of conventional concrete are scale-dependent due to the relative dimension of aggregates and the effects of strain energy release on fracture [24]. Such effects may be expected in additively manufactured concrete too, but are likely even increased due to the growth of the number of interfaces in larger specimens. For instance, to produce wider print objects, adjacent layers are typically deposited, creating not only horizontal interfaces (e.g., between stacked filaments in the height of the object) but also vertical ones (e.g., lying at the filament side between adjacent layers). To enable the study of scale effects, the Study Plan proposed mechanical characterization tests at two increasing levels of dimensional scale, corresponding to typical dimensions of specimens made of cementitious mortars (order of several centimeters for specimen width) or concretes (order of 1 to 1.5 dm for width), respectively.

Usually, specimens for characterization of traditional mortars or concretes are obtained by casting into formwork of small or even large dimensions. Obviously, this is not a suitable method for printing (printing into formwork is possible, but it was expected this would not realistically represent actual printed concrete in a free-form condition). Therefore, to obtain specimens with regular shapes/geometries (i.e., avoiding irregular sides due to filament characteristics) it was proposed that specimens were sawn from larger printed objects. Each side of a specimen would be sawn in order to be able to accurately determine the geometry and dimensions of a specimen and to exclude the effects of uneven (printed) edge surfaces. Alternatively, specimens could be core-drilled from printed objects, as this is common to determine the properties of existing structures.

Typically, a range of process parameters can be set to perform a printing session (nozzle velocities, output rate, pressures, layer offsets, output flows, layer thickness, layer interval time etc.). Considering the wide range of printing facilities used by different laboratories, these settings could not universally be prescribed. The laboratories were required to use their default process settings during printing, which they considered to provide satisfactory printing results. The settings that were assumed to be the most relevant were to be reported (e.g., type of mixer, material extrusion rate, print head travel velocity etc.). In addition to the default process settings and conditions, two deviating conditions were defined that were added as voluntary to the experimental program. 'Dev1' describes a process where the middle horizontal interface of a specimen is printed at a significant delay, resulting in a layer interval time larger than the expected cold joint formation threshold. The exact duration of the interval time was to be defined by the respective laboratory. 'Dev2', on the other hand, was related to the curing conditions and defines a deviation from the standard under water curing. Again, the respective laboratories were free to define the exact conditions of this deviation.

The standard minimum of results for each experimental series was set at 5, except for the mortar scale compression and splitting tension tests, for which the minimum was set at 9 as further explained in Sect. 4.

4 Instructions

4.1 Material and equipment

Specimens subjected to ILS mechanical testing were produced from different printing setups available at the various laboratories involved, differing from each other by mixing, pumping and extrusion-based printing equipment. These setups are commonly adopted in the current 3DCP practice, either at the laboratory scale or industrial applications by companies; hence, the ILS included this variety of printing setups to provide a comprehensive interpretation of the technological options. In terms of type of mixer, batch mixers (drum-type or pan-type) or continuous mixers (volume and time) were employed. For the pumping purpose, different types of pumps can be considered, such as piston, rotor–stator, and peristaltic ones. To transport the material from the pump to the nozzle, hoses of varying length and diameter are typically used. Both mixing and pumping equipment are part

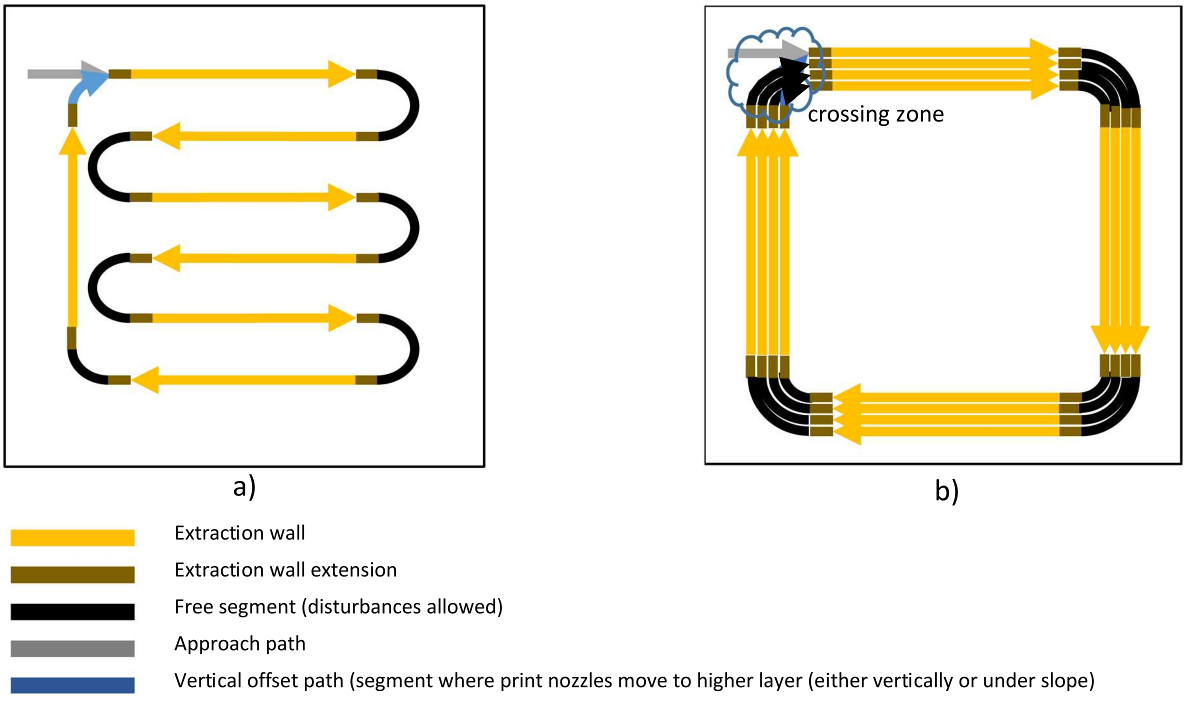

Fig. 1 Printing path options to produce print specimens in the mortar scale with **a** U-shape and **b** square shape

of a particular printer machinery which can be, for instance, of gantry, robotic arm, or delta type; they are characterized by a maximum size of the print region, type of extruder (screw, progressive cavity pump, piston), orientation (vertical or horizontal material discharge), shape (round, rectangular) and the size of the nozzle.

These and other material and facility characteristics that were expected to be potentially relevant to the results analysis, were to be reported in the results template distributed before the execution of the interlaboratory testing plan.

4.2 Specimen preparation

The reader is referred to the Study Plan [19] for full details. In general, specimens for mechanical testing were obtained from larger printed objects (Fig. 1)—containing extraction walls—fabricated with specific automated machinery. Cast specimens—representative of the same printing material—were also considered and produced for qualitative/quantitative comparison purposes. Irrespective of the type of mechanical test to be conducted, the specimen preparation procedure shared common features, here summarized:

- *Geometry* (*printed objects*): shapes are typically square, rectangular or U-shaped and made of several layers (both in the height and width direction) depending on the mortar/concrete scale. The total length of the shape generates a specific interlayer time which is dependent on the applied displacement rate of the nozzle.
- *Geometry* (*specimens*): cubic, prismatic or cylindrical shapes with different dimensions are considered in relation to (i) concrete/mortar scale; (ii) the type of mechanical test; and (iii) extraction procedures adopted from the straight walls of the print objects. For the dimensions of specimens, recommendations were given. However, it was allowed to deviate from these dimensions, as testing in various regions in the world is often based on codes or guidelines that follow similar principles but maintain modestly varying dimensions. For the mortar-scale specimens, however,

a) b)

Fig. 2 Examples of specimen preparations: **a** mortar scale print specimens protected against vapor evaporation and **b** free segments cutting after printing U- shapes

it was required to maintain a maximum of 2 adjacent filaments and not to increase the specimen size beyond that.

- *Extraction*: specimens were extracted from the 'extraction walls' of square, rectangular or U-shaped print objects by sawing and/or core-drilling depending on the concrete or mortar scale of the tests. For extracting the specimens by sawing or core drilling, different locations were chosen with respect to the height position of the specimen in the print object to analyze possible effects of the stacked layer weight during printing (see Sect. 4.5).
- *Environmental conditions*: in the laboratory, during the printing phase of the objects, the recommended temperature was T = 20 ± 2 °C with a relative humidity RH ≥ 70%. Both parameters are considered important for the print quality, therefore they need to be recorded at least at the start and end of each printing session.
- *Curing*: preferably, all specimens were tested at an age of 28 < days < 30. During this period, curing is differentiated between 'initial' and 'normal' condition; in particular, under the initial curing condition, the print objects should be protected against vapor evaporation (e.g., providing wet jute or alternative and covering with plastic foil, see Fig. 2a) for at least 24 h after printing. After the material has set sufficiently, the print objects can be stored under 'normal' curing conditions consisting in the immersion in tap water at a temperature of 20 ± 5 °C. Deviating conditions were not rejected a priori but were required to be reported. In addition to the default curing conditions, deviating conditions could optionally be tested as explained in Sect. 3. Such deviations could include the application of curing agents, water spray mist, or (on the contrary) unprotected curing.

4.3 Print object geometry and print paths

Each participating entity in the ILS was responsible for designing and programming the print paths for their print objects, taking into account their specific process constraints. However, the design of these paths needed to adhere to the guidelines outlined in the Study Plan (e.g., as in Fig. 1). In particular, the print objects were structured to include several straight walls, i.e., 'extraction walls', from which experimental specimens were derived. Adjacent to these walls were 'extraction wall extensions', which are straight wall segments equal to or longer than the minimum specimen dimension (40 mm for mortar-scale and 100 mm for concrete-scale specimens). The printing path in these extensions remained continuous and free from any disturbances like cornering or nozzle height adjustments, which are planned outside of these areas (Fig. 2b).

The print path ensured uniform layer interval times for both vertical and horizontal interfaces across all extraction walls, avoiding the formation of cold joints, though this is less of a concern with slower-curing print materials. However, a deviation in the specimen preparation (Dev1) could be pursued during the printing process which would be paused between the printing of 2 subsequent layers to achieve a weaker interface in the middle of the designated specimens.

In designing the print path, the direction of printing was to be kept consistent across adjacent layers, both vertically and horizontally. The print path design included vertical and horizontal layer offsets, with recommended values being the nominal layer height for vertical offset (or slightly less, depending on the process) and 90% of the nominal layer width for horizontal offset (e.g., 45 mm for a 50 mm layer width).

The print filaments had to have a minimum nominal width b ≥ 21 mm, so that when assuming a 10% horizontal overlap, a 40 mm wide specimen consisted

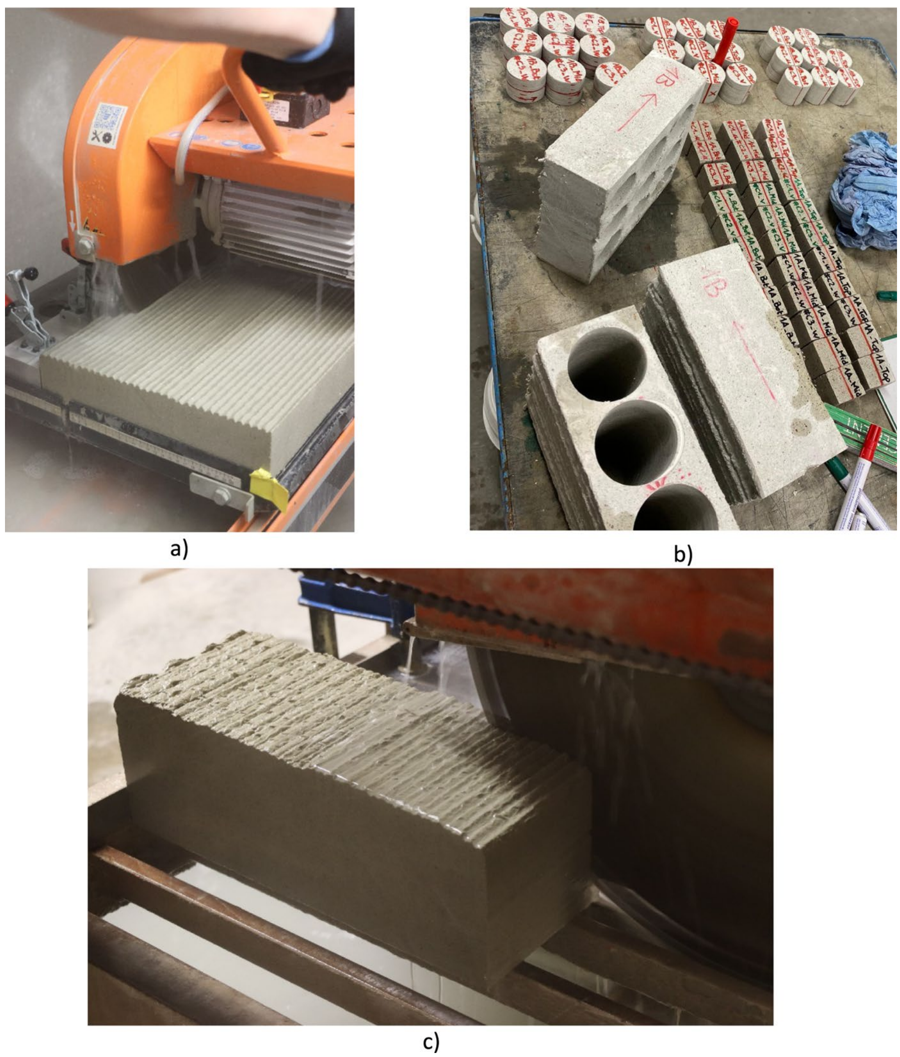

Fig. 3 Specimen extraction by means of **a** sawing of the extraction walls and **b** core drilling; **c** details of sawn specimens

of no more than 2 adjacent layers when the interface is in the middle.

4.4 Cutting and sawing

Differently from traditional cast concrete, print specimens can be obtained from cutting and sawing operations. In particular, for storage convenience, large print objects can be sectioned into smaller, typically straight, parts. This is accomplished by cutting the concrete before early setting, or by sawing once it is in the early stages of hardening. All types of cuts are made outside the extraction walls (e.g., as in Fig. 3a) and their extensions, taking special care not to disrupt the integrity of the extraction walls. Prior to testing, the print objects, or the parts pre-cut or sawn before setting, are further prepared to obtain the required dimensions. This involves sawing and/or core-drilling (Fig. 3b), using appropriate equipment and following the guidelines specific to each mechanical test type. Unless specified differently in the test specifications, specimens are ideally extracted from the central half of the print object's height. In addition, to guarantee a symmetric condition in the layered structure of the specimens, each one is taken from a print object in such a way that a nominal horizontal interface aligns with the specimen's mid-plane (see Fig. 3c to highlight this feature). Similarly, when relevant, a specimen is extracted to ensure that a nominal vertical interface aligns with the mid-plane of the specimen.

4.5 Execution of tests

The specimens obtained through the procedures described above and reference cast ones were tested according to the appropriate test specification documents that are part of the Study Plan. As a general approach, the tests are based on existing standards for mortar and concrete materials. However, due to the particularities of extrusion-based printing (e.g., presence of interfaces, anisotropy etc.), some modifications were implemented. In particular, the following test types were considered and include the main changes listed below; detailed descriptions are reported in the Study Plan.

- **Compression:** the tests are carried out on specimens that are sawn or core drilled from hardened print objects. The recommended dimensions for mortar-scale specimens were length x width x height = 40 × 40 × 40 ± 1.0 mm for cubes and height = diameter = 50 mm ± 1.25 mm for cylinders. The tests were performed in a load-controlled fashion at a recommended rate of 2,400 ± 200 N/s. Contrary to some codes (such as the EN 196-1 for mortar [25]), specimens for the compression test are not obtained from the remaining halves of broken flexural specimens but they are extracted as cubes from a print object. Moreover, the experimental tests include sets of 3 specimens taken from 3 different height locations in the print object (bottom, middle, top, as illustrated in Fig. 4) to evaluate the homogeneity/not homogeneity of the

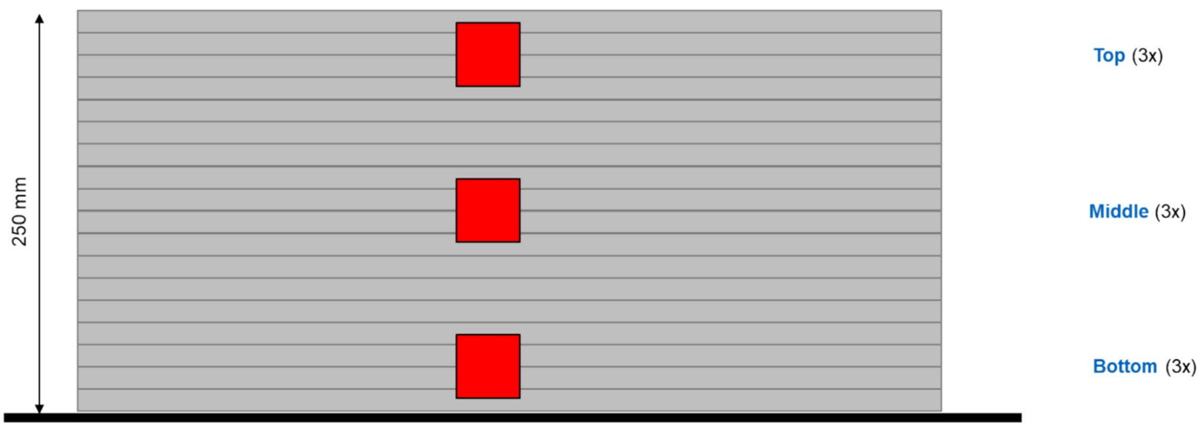

Fig. 4 Positions to consider for specimen extraction along the height of the extraction walls

compression properties by varying the height of extraction.

These specimens extracted from different heights were analyzed both as small separate sets of 3 and jointly as sets of 9 specimens. The effect of printing direction is analyzed by executing the uniaxial compressive tests in the 3 orientations u, v, w.

- **Elastic modulus**: the test aimed to determine the stabilized secant modulus of elasticity in compression of prismatic and cylinder-shaped specimens in the mortar-scale and concrete-scale category. The reference code provision for test execution is EN 12390–13: 2021 [26]. However, some modifications were implemented. The dimensional requirements for specimens consist in adopting the ratio between the specimen length L and the diameter d (or side in the prismatic shape) in the range $2 \leq L/d \leq 4$. This results in recommended mortar-scale dimensions of base × height = (40 × 40) × 80–160 mm for prisms and diameter × height = 50 × 100–200 mm for cylinders. The load is applied and removed in cycles at a rate of 0.6 ± 0.2 MPa/s. The modus is computed from printed specimens in 2 different orientations: u and w. Furthermore, in the E-modulus test it is required to predetermine the compressive material strength in order to be able to define the compression load during E-modulus testing as a percentage thereof. In deviation from the EN 12390-13:2021, it was allowed to use the compression test results (which use a different specimen geometry) for this, to avoid unnecessary additional testing. At the end of the E-modulus test, a specimen is compressed to failure. This provides an additional compression strength result. In [21], these values are compared to results from the actual compression test.

- **Flexure:** both a 3-point and a 4-point bending set-up were considered to determine flexural properties of printing materials. Mortar-scale specimens had recommended dimensions: width x height x length = 40 × 40 × 160 mm. The tests were performed in a load-controlled fashion at a rate of 50 ± 10 N/s when the recommended dimensions were used, or recalculated to a corresponding maximum flexural stress rate of 0.14 ± 0.028 MPa/s. Different orientations (i.e., generated by the interface position with respect to the load direction) are also considered for fully characterizing the flexural properties of the printing material (u.w, v.u, w.u for 3-point bending, u.w for 4-point bending).
- **Splitting**: for splitting tensile tests, both cubic and cylinder-shaped specimens were considered in the mortar-scale and concrete-scale category. The proposed procedure deviates from the standard EN 12390–6 for several aspects, amongst others because that standard prescribes cylindrical specimens only. The experimental tests include three sets of specimens taken from 3 different height locations in the print object (bottom, middle, top) to evaluate the homogeneity/not homogeneity of the tensile properties by varying height of extraction, similar to the compression specimens. Three different orientations were also considered for fully characterizing the splitting properties of the printing material. The existing convention to define specimen-to-load orientations had to be expanded to properly define splitting tension specimens (further detailed in the Study Plan).
- **Uniaxial Tension**: uniaxial tension tests are carried out on prismatic or cylindrical specimens in the mortar-scale and concrete-scale category and in 2 different orientations: u and w.

Figure 5 shows an entire set of specimens at the mortar scale after the execution phase. A practical evaluation of the applied experimental methods can be found in Sect. 7.

5 Response

5.1 Contributions and content

The study yielded a vast response. After processing (see Sect. 6.2 below), 34 contributions submitted by 30 laboratories from 19 countries remained (Germany: 5; China, Czech Republic, France: 3; India: 2; Australia, Belgium, Brazil, Canada, Chile, Italy, Latvia, the Netherlands, Slovenia, South Africa,

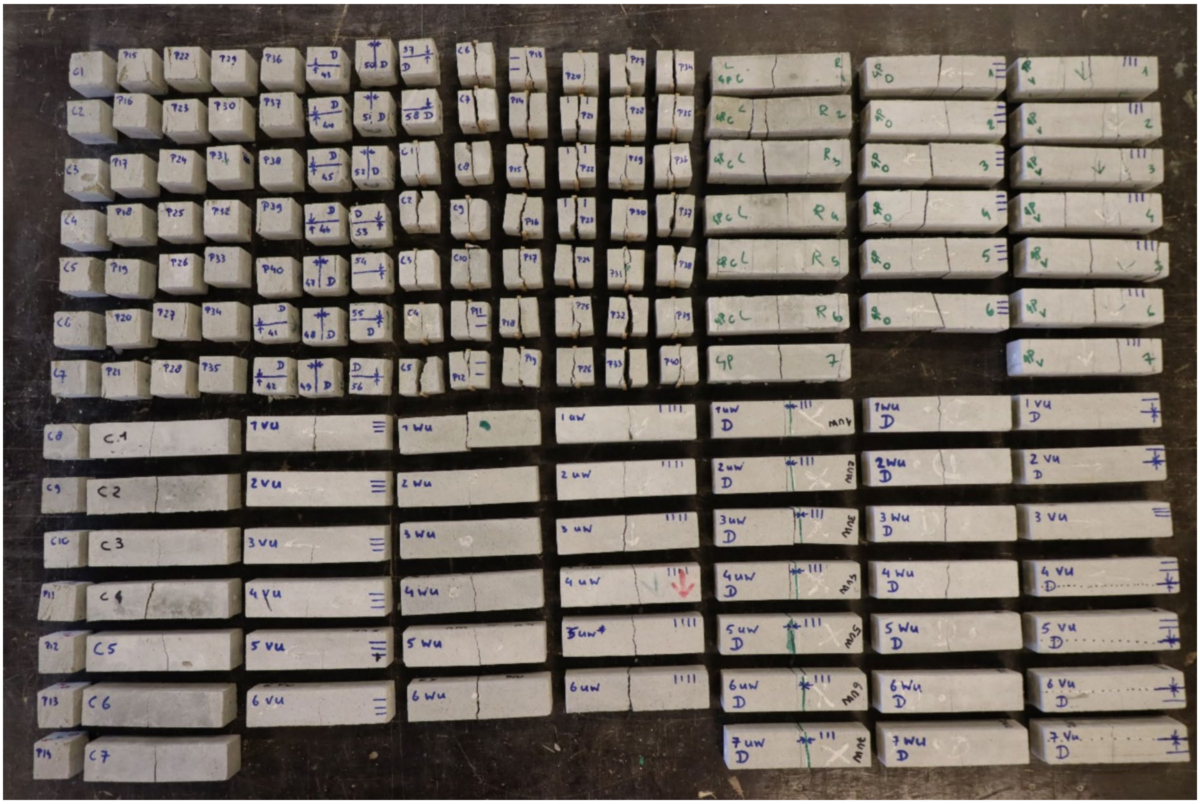

Fig. 5 Overall view of tested specimens at the mortar scale

Switzerland, Thailand, Turkey, United Kingdom: 1). Appendix A lists the participating laboratories in alphabetical order. A 'contribution' consists of the experimental results (at least from the mandatory tests) on one specific material printed on one specific facility, albeit not necessarily in the same session or on the same date.

The data were collected using a predesigned spreadsheet template that was filled out and returned by the participating laboratories. The experimental results template allowed for additional comments. Some laboratories also included photographs of specimens and/or experimental set-ups, or additional descriptions in separate files. The 34 contributions contain approximately 5,000 individual specimen test results. To allow an efficient analysis of such an extensive set of results, a database was created that can be queried for results for specific parameter combinations. When entering the data into the database, individual laboratories were occasionally approached to clarify any possible unclarities in their response. The database is set up so that additional data may be added in the future and will be made available for additional queries and analyses by the community. The approach to data processing and analysis is extensively described in a separate publication [20].

The overall response is summarized in Fig. 6 in which type of test (colored bars) and corresponding number of samples are reported for each ILS participating laboratory, distinguishing between concrete and mortar scale. Mortar scale testing is included in 33 out of the 34 contributions, while concrete scale testing is included in 8 contributions (i.e. 1 contribution only contains concrete scale specimens, while 7 contributions contain both mortar scale and concrete scale specimens from the same laboratory).

The compression and flexural bending tests have been performed most as these were compulsory for participation in the interlaboratory study, while the other experiments were optional. The splitting tension test was also performed frequently, probably due to the relatively modest effort required for its

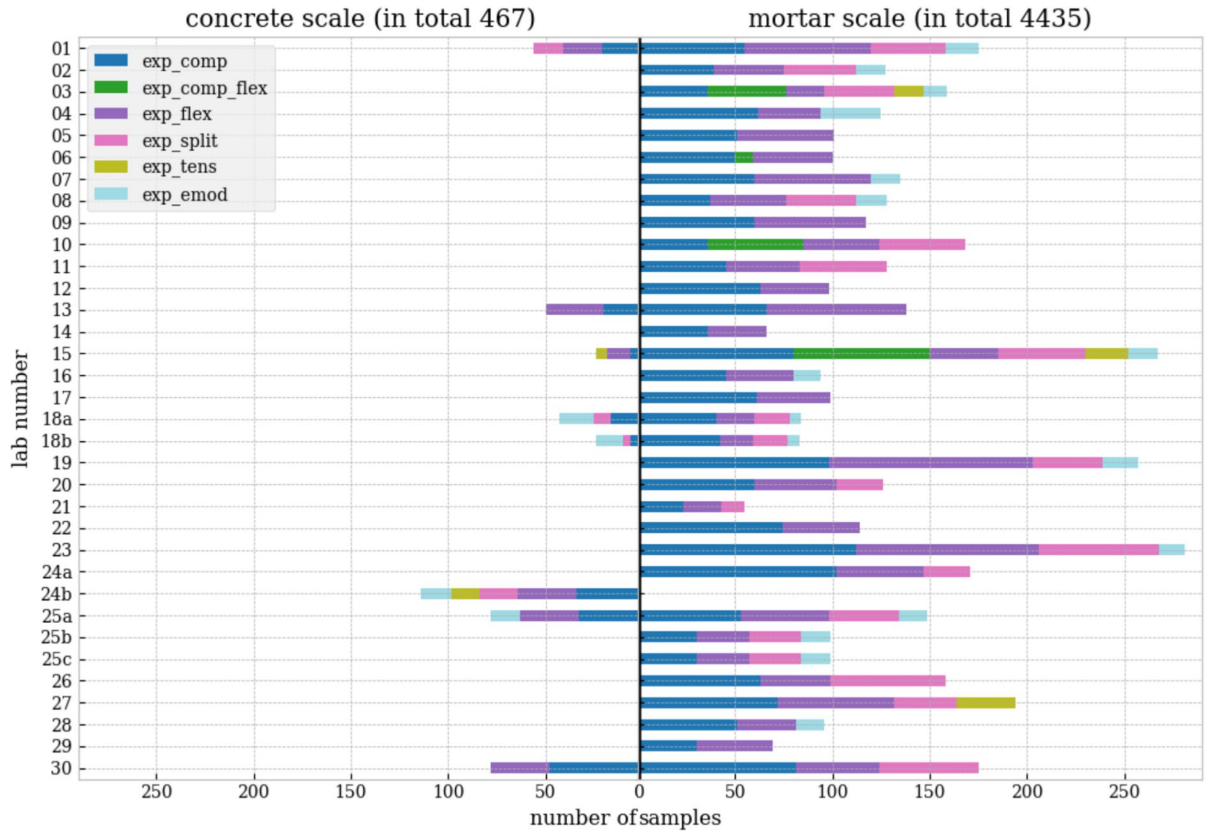

Fig. 6 Overall response of the participating laboratories, showing the number of tested samples for mortar (right side) and concrete (left side) scale as well as for each test type executed (different colored bar). Here, 'exp' indicates experimental results, while 'comp', 'comp_flex', 'flex', 'split', 'tens', and 'emod', indicate compression, compression on remaining halves from flexural testing, flexural, splitting tensile, uniaxial tensile, and E-modulus, respectively

execution. The E-modulus has been executed in a smaller, but still significant number of contributions. This is important, as hitherto most studies focused on strength and very little data on stiffness of printed concrete has been published, even though it is an important parameter for structural analyses and modeling. Furthermore, the E-modulus test also gives a compressive strength value as specimens are loaded to destruction at the end. These values can be compared to the compressive strength of cubes to obtain an indication of aspect ratio effects, being equal to 2:1 and 1:1, respectively.

According to the Study Plan, the compressive tests were performed on separately produced cubes or cylinders. However, a few laboratories have also compressively tested the remaining halves of flexural specimens after 3-point bending ("exp_comp_flex" in the legenda of Fig. 6), as it is common for mortar testing. These results can be used to evaluate whether they provide a sufficiently accurate compressive strength and thus whether this procedure may be followed in the future to obtain compressive strength data.

The uni-axial tensile test has been performed least (in 3 contributions in the mortar scale and 2 contributions in the concrete scale), possibly due to its complexity in specimen preparation and in its execution.

Generally, the testing orientations of printed specimens prescribed in the Study Plan were all followed (3 for compression, 3 for 3-point bending, 1 for 4-point bending, 3 for splitting tension, 2 for uni-axial tension, and 2 for E-modulus). This allows an extensive analysis of the effect of loading

Table 2 Type of printing approach in combination with type of mortars adopted in the interlaboratory study

Mortar/mixing	Continuous	Batch	Total
Commercial	7	3	10
Self-prepared	3	21	24
Total	10	24	34

orientation. In a few cases other orientations were tested due to mistakes.

Deviating process parameters were applied in 15 contributions: 10 contained deviating curing conditions (Dev2), 3 had a prolonged layer interval time (Dev1), while 2 contributions featured both deviations.

In terms of sample preparation, in 28 contributions only sawing was used to obtain specimens from printed objects. In 5 contributions, both sawn and core-drilled specimens have been tested, while in 1 contribution contained waterjet-cut and core-drilled specimens.

5.2 Characteristics of applied facilities and materials

Even within the set scope as outlined in Sect. 2, the characteristics of the printing facilities and materials that were used by the various laboratories vary considerably. In 10 contributions, commercial 3D printable mixtures were used, while they were self-prepared in 24 instances. The material was also continuously mixed in 10 contributions, and batch-mixed in 24 cases, but not in the same ones, as shown in Table 2.

With regard to the material concept, the single component systems were heavily prevalent, making up 31 of the contributions. Two others were two-component systems, and one was a three-component system. Although commercial multi-component material systems exist, in this study they were all self-prepared.

The maximum aggregate size in printable mixtures ranged from 0.25 to 16 mm (no data provided in two cases)—where the largest is an exception, though. Most mixtures use rather small maximum aggregate sizes, with 13 laboratories using aggregates between 1 and 2 mm of max size (mainly for mortar but also for concrete scale); about 2/3rd is below 2.0 mm. However, a significant portion of 1/3rd uses medium sized aggregates in the range of 2.0–8.0 mm. The overall distribution of aggregate size for the participating laboratories and for mortar and concrete scale is reported in Fig. 7.

Based on the printing facilities and materials above described, the ILS required the material

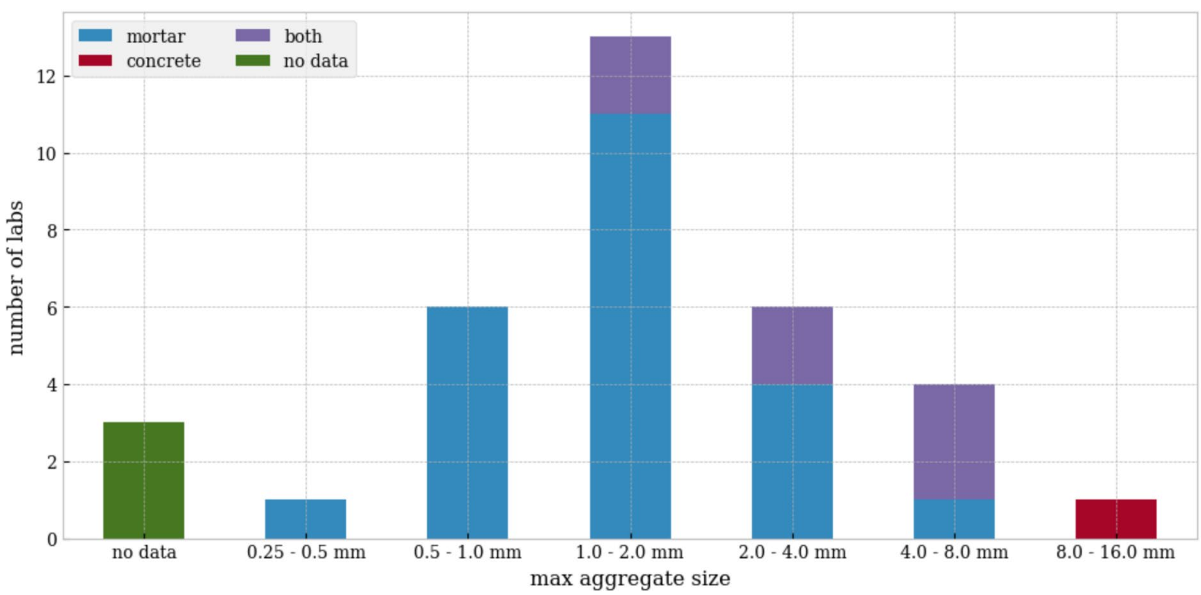

Fig. 7 Aggregate size used in all the printable mixes for the interlaboratory study. 'Mortar' and 'concrete' indicate this material was only used for mortar scale and concrete scale testing, respectively, while 'both' indicates this material was tested on both scales

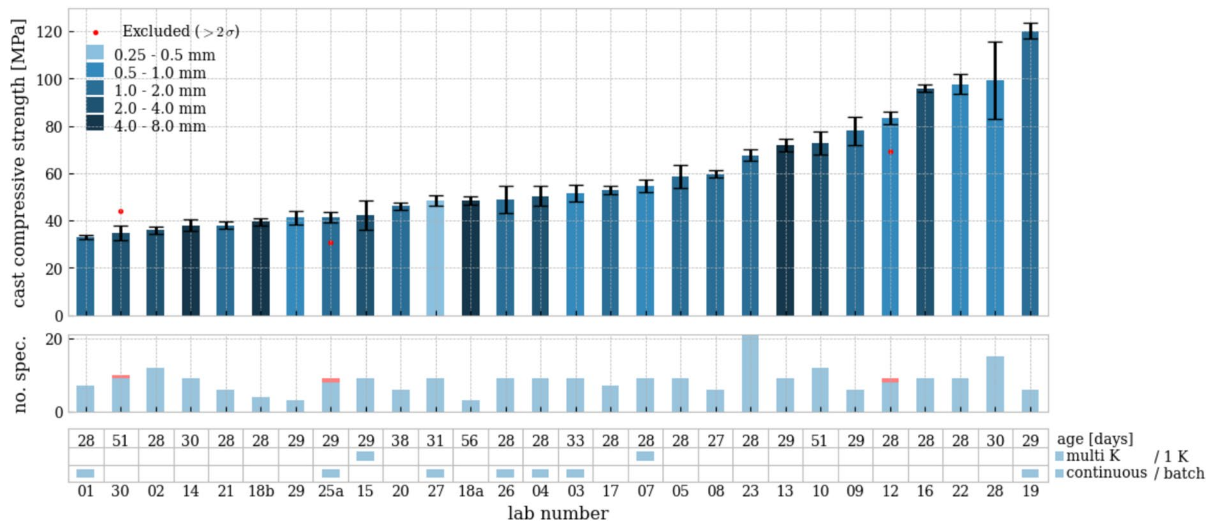

Fig. 8 Compressive strength results for cast specimens in ascending order showing aggregate size as different bar color; number of tested specimens, age, mix component number and material supply system are specified below the histogram for each laboratory. Red dots correspond to excluded results according to exclusion rules

characterization in compression in the cast preparation option (cubic specimens; cylinders were not considered at this stage), to analyze differences with respect to the 3DCP technology. Figure 8 shows the average compressive strength for cast specimens at mortar scale, an age of > 20 days, and default process parameters, of each contribution organized from lowest to highest value. It shows the contributions cover a considerable range of compressive strengths (between 35 and 120 MPa with 2/3rd of contributions below 60 MPa), with experimental variation which varies considerably in some cases. The maximum aggregate size is also indicated by the color of the histogram bar according to the size ranges of Fig. 7. For each laboratory, the number of tested specimens, curing age, component system and material supply approach are specified below the histogram. The distribution of results shows that the cast compressive strength is not strongly correlated to either one of these characteristics, although there may be a slight skewer towards smaller maximum aggregate size for stronger materials. It should be noted that for the sake of completeness—at this stage of the analysis—also longer ages were included in the compressive strength distribution of Fig. 8 (e.g., > 50 days). However, in the following discussions and considerations, some exclusion rules had to be defined and applied in order to provide reliable comparisons and conclusions. For instance, the red dots in the Fig. 8 represent the excluded test results—named 'outliers'—corresponding to a deviation from the average compressive strength value (of a specific laboratory) greater than 2 times the Standard Deviation.

Moving from casting/pouring approach to the 3D concrete printing process, we first analyzed the overall settings adopted by the different laboratories. Specifically, when observing the printing facilities and settings, we again observe a considerable range of parameter values adopted by the different laboratories. In almost 1/3rd of the facilities, the material is fed into a hopper directly over the print head or mixed at the print head and deposited from that with a negligible transport length through hoses or pipes (Fig. 9). Most facilities where the material is mixed at a distance, the hose is between 5 and 10 m long, but shorter (0–5 m) hoses as well as longer ones (10–20 m) are also used in a considerable number of contributions. Very long hoses (> 20 m) were reported only in two cases. The hose length can be an influencing parameter due to after-mixing effects, induced shear, compaction, void formation, segregation, friction and material warming.

Except for 1 contribution where the nozzle is pointing backwards in the negative u-direction, the deposition direction of all applied nozzles (33 times) is downwards, in the w-direction. The nozzle travel

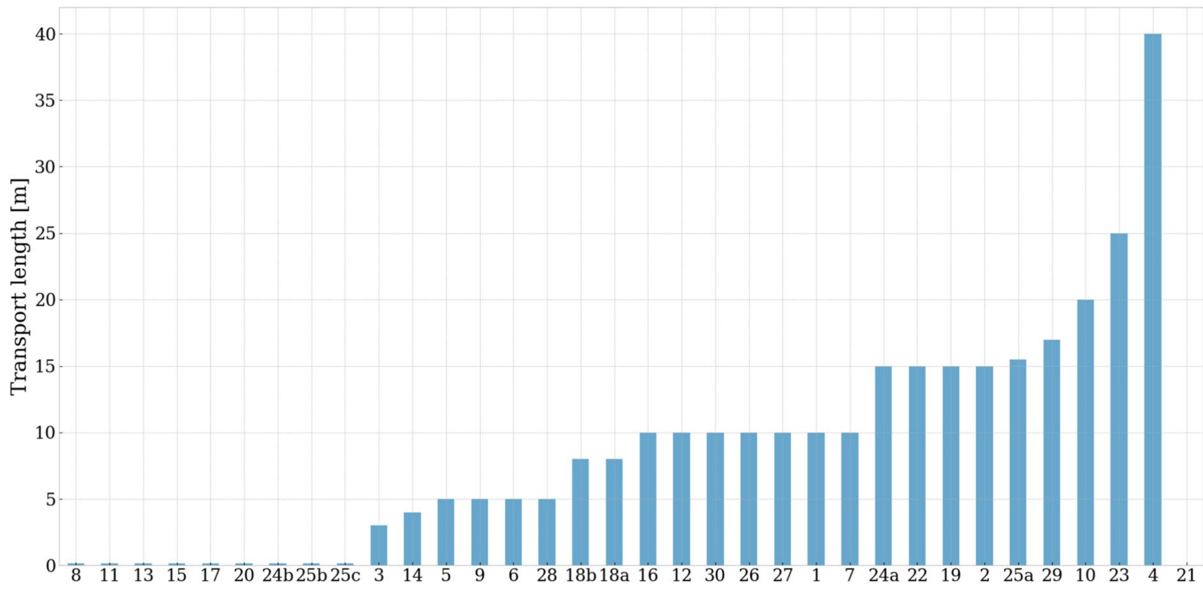

Fig. 9 Distribution of transport length over the different laboratories (ascending order); empty bars on the right correspond to labs with no or incorrect data provided

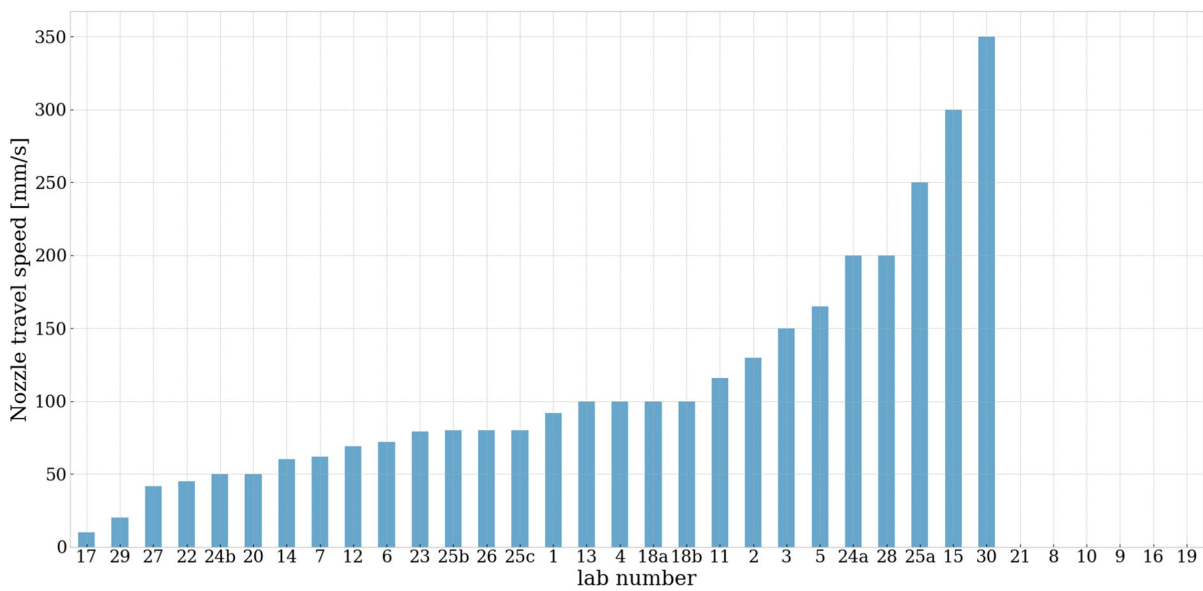

Fig. 10 Distribution of nozzle travel speed over the different laboratories (ascending order); empty bars correspond to labs with no or incorrect data provided

speed also shows a wide range of variation between the laboratories, as shown in Fig. 10; more than 50% of the printing facilities are below the limit of 100 mm/s of nozzle speed whereas there are very fast printing systems which are able to move at a velocity more than three times faster (> 300 mm/s).

Round nozzle mouths are typically used, but rectangular ones can also be found (six in total).

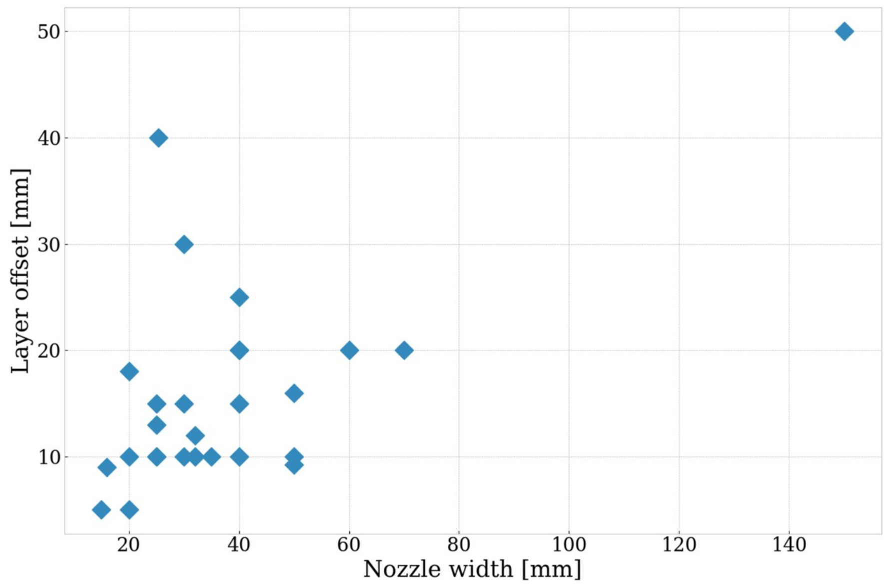

Fig. 11 Correlation between nozzle width and layer offset parameters adopted by the different laboratories

Therefore, the nozzle cross-section area dimensions vary considerably, from 177 to 7500 mm^2, and fairly evenly distributed in between these extremes, with 4 times 314 mm^2, 7 times around 500 mm^2, 5 times 707 mm^2, and 4 times 1257 mm^2. Figure 11 plots the nozzle width (i.e., the dimension determining printed layer width) against vertical layer offset height and shows there is no clear relation between these parameters, positively nor inversely. In particular, when the nozzle width is < 40 mm, most of the labs adopted layer offsets between 10 and 20 mm; for larger widths, the layer heights are highly variable. Similarly, the product nozzle section area * vertical layer offset could be plotted against nozzle travel speed, but this too would not result in a clear correlation. This indicates that the pump flow rate varies significantly between facilities (although this property was also directly queried in the results template, most laboratories did not provide data here, so it could not be compared directly).

The wide variety of material and facility characteristics covered by the submitted contributions indicate that any conclusions of this study will not be limited to a specific type of material or printer. On the other hand, this variation may present a challenge in the evaluation of the outcomes.

6 Experimental results

Due to the variety of the properties of the materials that have been used (see Sect. 5.2), an absolute quantitative comparison of results is not meaningful to study the effects of printing process parameters and highlight differences between laboratories. Rather, it was opted to use the different strengths and E-modulus of cast samples, produced and cured under default conditions and tested after 21 days or more, as reference values and present the other results as a percentage relative to those. The age difference between cast and printed specimens could not be more than 11% (this coincides with the initially prescribed testing range of between 28 and 30 days). This way, the general effects of the print process on the mechanical properties can be analyzed over multiple combinations of material and print facility.

As indicated, the interlaboratory study yielded a large number of mechanical testing results that are presented and analyzed in detail in the associated publications [21] and [22]. This includes, amongst others, a discussion of outliers. Below, only a few of the most essential results are reported, namely the compressive strength, 3-point flexural bending strength and E-modulus for default printing and curing conditions, at mortar scale. Here, no detailed analysis and additional exclusion of outliers is performed. The same exclusion rules as discussed for the cast specimens' results in Fig. 8 are applied for the absolute values of

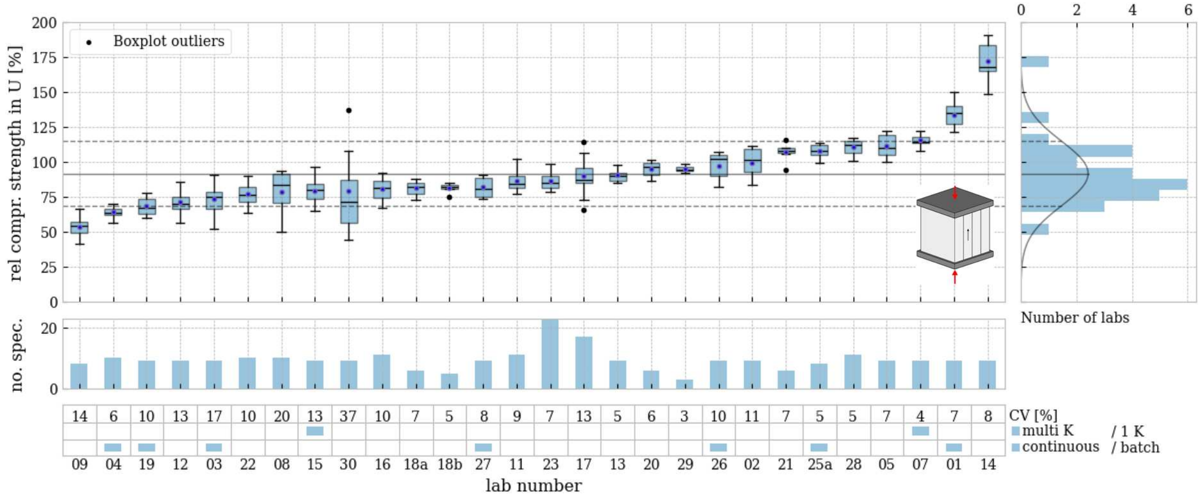

Fig. 12 Relative compressive strength results (print over cast, in percentage) in the U direction in ascendent order for each laboratory, represented as box-whisker plots. The additional blue dot represents the individual lab average. The table at the bottom includes the number of specimens used to compute the average, coefficient of variation (CV as percentage), component system and material supply approach. The bar diagram on the right presents the histogram and normal distribution of laboratory averages. The layout of Figs. 13, 14, 15, 16, 17, 18 and 19 follows the same format

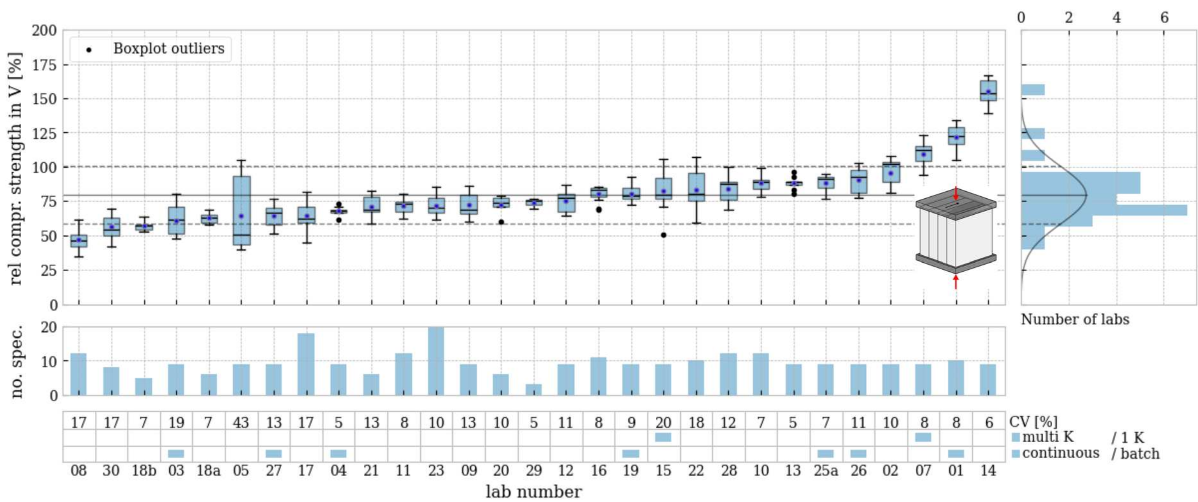

Fig. 13 Relative compressive strength results (print over cast, in percentage) in the V direction in ascendent order for each laboratory. Further explanation provided with Fig. 12

cast and printed specimens. Afterwards, the relative values are computed by division with the lab's averaged cast strength.

6.1 Compression

The relative compressive strength of printed concrete specimens at mortar scale (cast and print—sawn cubes, default conditions, older than 20 days) is presented for orientations u, v and w in Fig. 12, Fig. 13, and Fig. 14, respectively, and reported in ascending

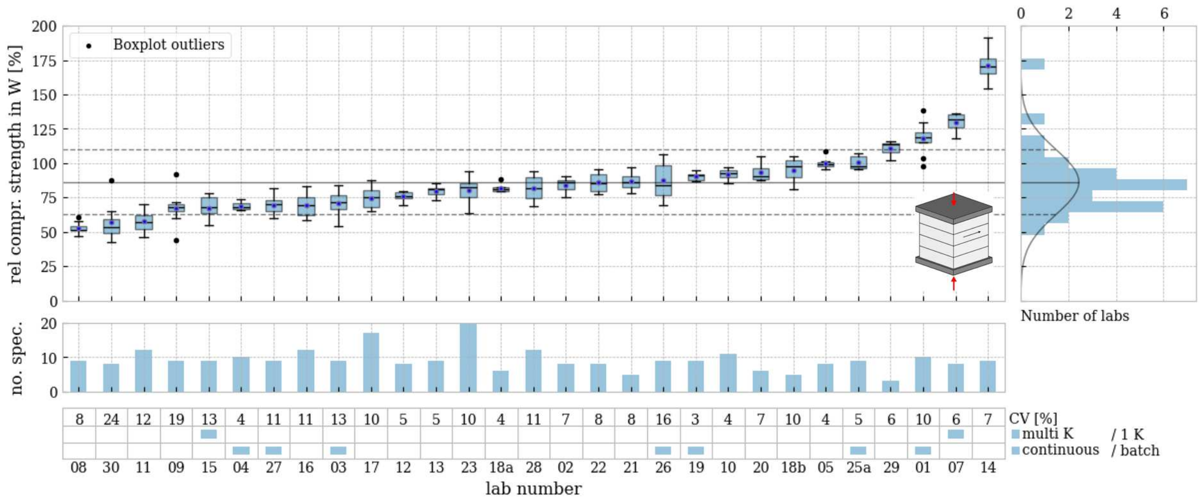

Fig. 14 Relative compressive strength results (print over cast, in percentage) in the W direction in ascendent order for each laboratory. Further explanation provided with Fig. 12

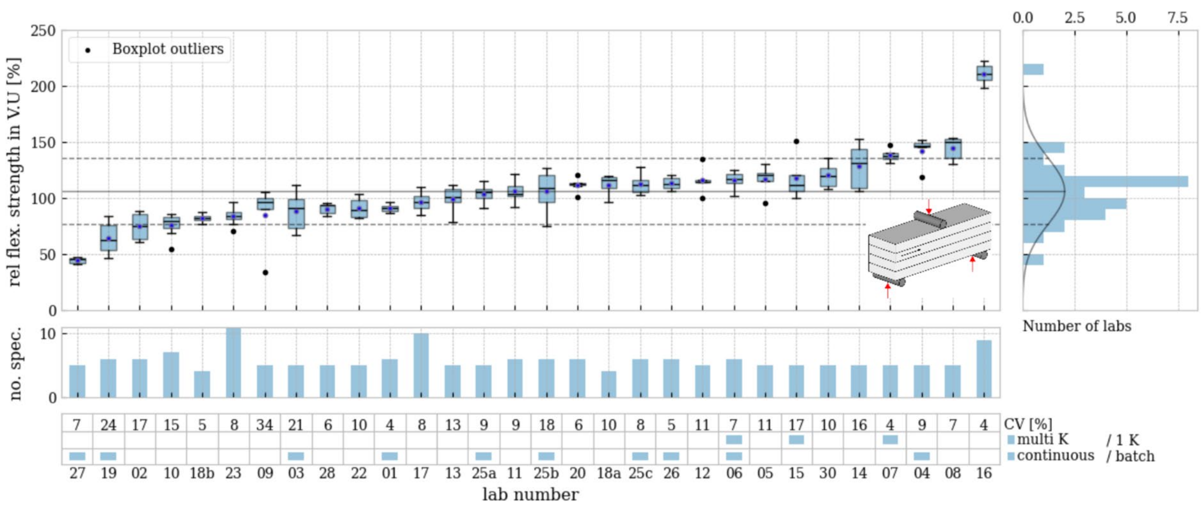

Fig. 15 Relative flexural strength results (print over cast, in percentage) in the v.u direction in ascendent order for each laboratory. Further explanation provided with Fig. 12

order. The graphs show the results of individual contributions in box-plot style, i.e. with the median as a black line in the box that indicates the upper and lower quartile and the whiskers giving the maximum and minimum value of the individual specimens. In addition, a blue dot shows the mean value, to which the contributions are ordered. The overall mean value of all contributions is given by the continuous horizontal black line, while the dashed lines give the + and −1 standard deviation. The table below the histograms of the results reports the number of specimens used to compute the average, coefficient of variation (CV as percentage), component system and material supply approach. The bar diagram on the right presents the histogram and normal distribution of laboratory averages. In Appendix B, the mean values of the laboratory results are presented in tabulated format organized by laboratory for all experiments and orientations presented in Figs. 12, 13, 14, 15, 16, 17, 18 and 19.

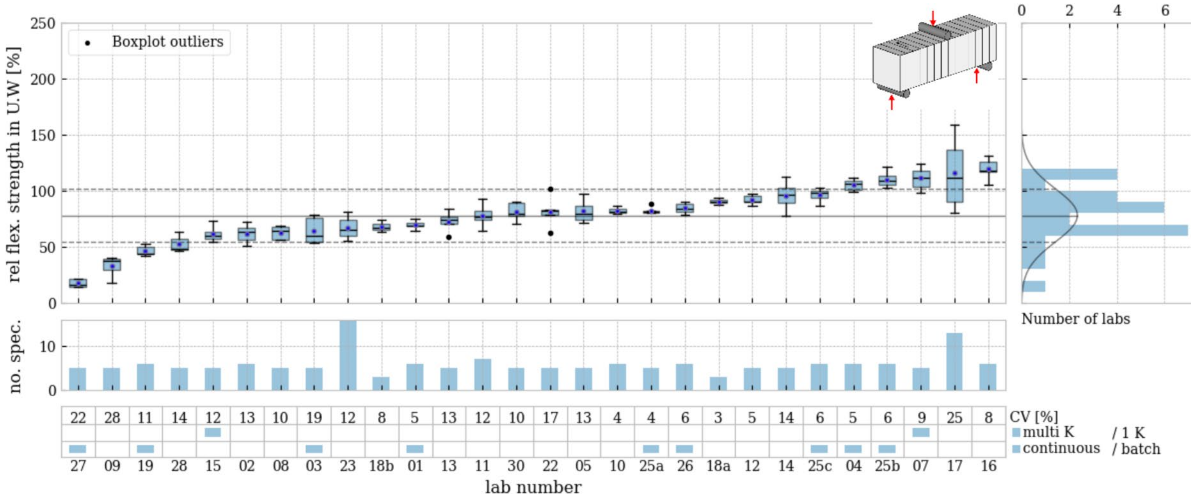

Fig. 16 Relative flexural strength results (print over cast, in percentage) in the u.w direction in ascendent order for each laboratory. Further explanation provided with Fig. 12

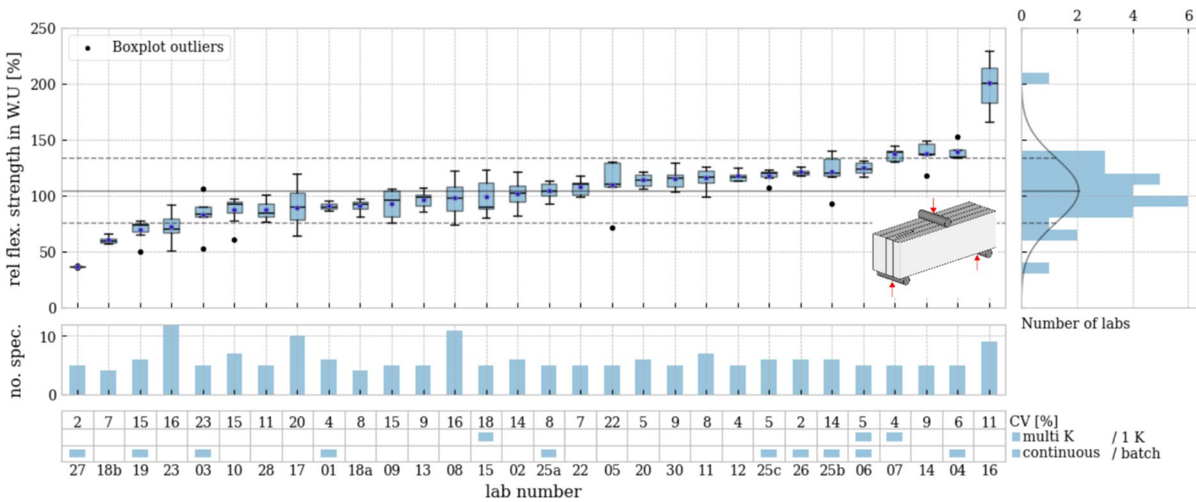

Fig. 17 Relative flexural strength results (print over cast, in percentage) in the w.u direction in ascendent order for each laboratory. Further explanation provided with Fig. 12

On average, the strength of printed specimens in all three orientations is lower than the cast specimen strength. For the u-orientation the relative compressive strength reaches approximately 90% of the cast counterpart, while the v-orientation reaches around 80% and the w-orientation reaches near 85% on average. The scatter, however, is considerable, with some contributions reaching average strengths of only $\leq 60\%$, while others achieving $\geq 100\%$ (in some cases far above). The relative order of contributions is mostly similar for the different orientations, although there are some exceptions (e.g. contribution 19 performs relatively better for orientations v and w than for orientation u, see Sect. 6.4 for further discussion).

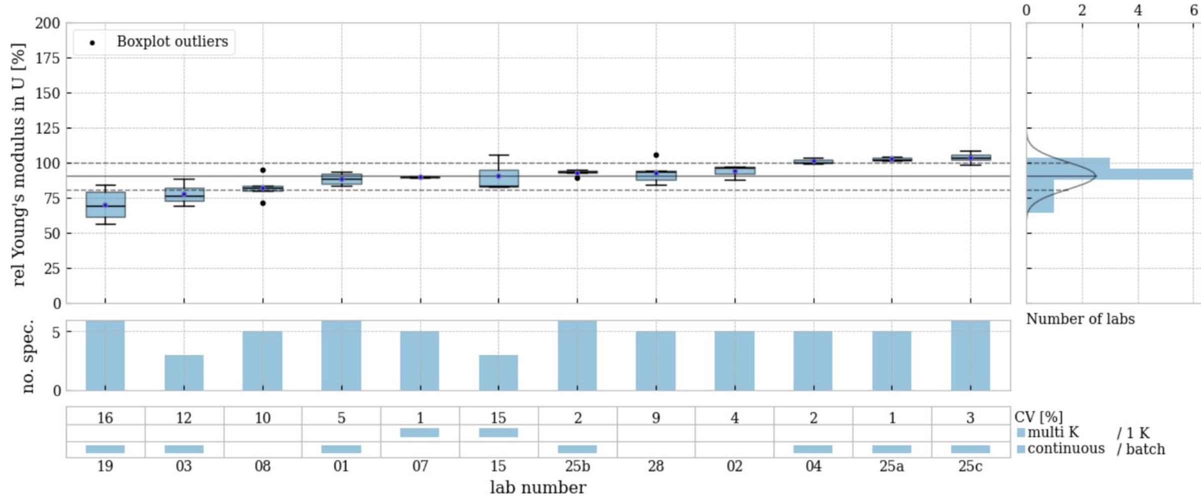

Fig. 18 Relative elastic modulus in compression (print over cast, in percentage) in u direction in ascendent order for each laboratory. Further explanation provided with Fig. 12

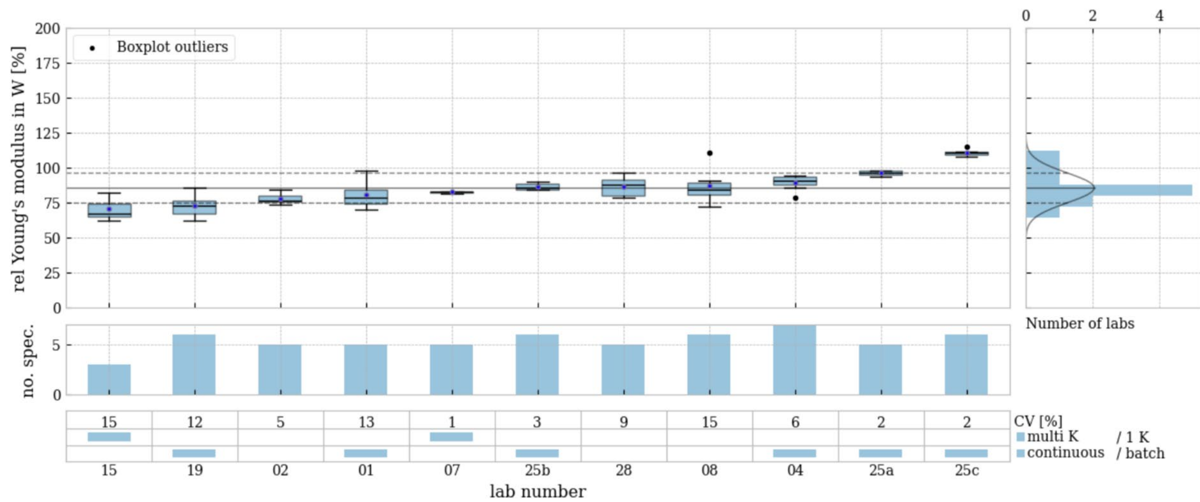

Fig. 19 Relative elastic modulus in compression (print over cast, in percentage) in w direction in ascendent order for each laboratory. Further explanation provided with Fig. 12

6.2 Flexural bending, 3-point

The relative flexural bending strength (3-point bending) of printed concrete specimens at mortar scale (default conditions, older than 20 days) is presented for orientations v.u, u.w, and w.u in Figs. 15, 16, and 17.

The strength for the v.u and w.u orientations in flexural bending – on average over all contributions – exceeds the cast specimen strength by around 5%, with some contributions reaching strengths of > 140%. This may not have been expected in itself but is particularly remarkable given that in none of the compression orientations an average of > 100% of the cast strength was found. Nevertheless, it should be noted that in some contributions, the average strength is significantly lower for printed samples, reaching 70% or less. Within single contributions, consistency is not automatic. In contributions 1a and 13a for instance, the relative strength in orientations v.u and w.u is very similar, but for contributions 2a and 11a there is a difference of 20% or more (also see Sect. 6.4).

Expectedly, the strength of specimens tested in the u.w orientation is significantly lower than that of cast specimens, because the layer interface is loaded in tension in this orientation. The average over the contributions reaches almost 80% of cast specimen strength. However, also here considerable differences between contributions are found, with some scoring dramatically low, while 5 contributions even exceed the cast specimen strength.

6.3 E-modulus

The relative E-modulus in compression of printed concrete specimens at mortar scale (sawn specimens, default conditions, older than 20 days) is presented for orientations u and w in Figs. 18 and 19. Similar to the compressive strength results, the compressive E-modulus averaged over the contributions was found to be lower for the printed specimens than for cast ones. The average for the w-orientation was 86%, while that for the u-orientation was 91%, indicating that the layer interface not only generates a lower tensile strength than the bulk material, but also a lower stiffness.

6.4 Analysis

It may be expected that the deviation of properties of printed specimens from cast ones (i.e. the ratio between properties from cast and printed specimens, on which Figs. 12, 13, 14, 15, 16, 17, 18 and 19 are organized) would exhibit some consistency in different orientations and different test methods. However, it was already noted in Sects. 6.1 and 6.2 that this may not be the case as some contributions appear in different positions in the ascending order. To analyze this further, Fig. 20 presents the relative properties from compression (3 orientations), E-modulus (2 orientations), and flexural (3 orientations) testing obtained from 8 laboratories that performed all these tests, normalized to the mean relative properties obtained from all laboratories minus 1 (i.e. the 0 horizontal represents the normalized mean over all contributions: if a property has a value of 0.1, this indicates the ratio between cast and printed specimens was 10% higher than the overall mean ratio for all contributions; if the overall average ratio was 80%, than it was 88% in this contribution). A review of these results shows little consistency, particularly when different types of tests are compared, but also between different orientations within one test type.

Consider for instance the results of laboratory 1. In compression (blue bars), the strength ratio of cast to printed exceeds the overall mean significantly (by 37% to 54%), while in flexure (red-brown bars), on the other hand, this ratio is about −11% to −14%, i.e. less than the overall mean. The results of laboratory 8 show significant variations between different orientations. For instance, in compression u-orientation, the strength ratio of cast to printed is −15% compared to the overall mean, while for the v- and w-orientation it deviates much more (−41% and −39%). The relative flexural strength in the v.u-orientation far exceeds the overall mean (36%), while the other 2 orientations both score below the overall mean (−20% and −6%). Similar observations can be made, to a greater or lesser extent, for most of the presented laboratory results in Fig. 20. Query ID="Q6" Text="Kindly check and confirm Figures and tables citations are correctly identified. Please note that figures and tables should be cited in ascending numerical order in the text and should be inside the main body of the text."

Following conventional understanding of the strength of concrete, where flexural strength and E-modulus are both related to compressive strength, one would expect high relative properties in one test to correspond to high relative properties in another. This, however, does not seem to be the case. It is suggested the printing setup and the properties of the interlayers (in turn determined by a range of parameters including the interlayer time) contribute significantly to the discrepancies between the tests.

When furthermore comparing material and print facility characteristics such as absolute material strength (cast), maximum aggregate size, or transport length to the relative deviations between print and cast material, no credible correlation could be established, e.g. a long transport length does not consistently result in a higher or lower relative strength of printed material versus cast, than a short one.

On the other hand, extensive data analysis presented in [21] and [22] shows that, when treating the overall results of each laboratory as an individual data point and after performing certain statistical procedures to eliminate outliers, certain correlations

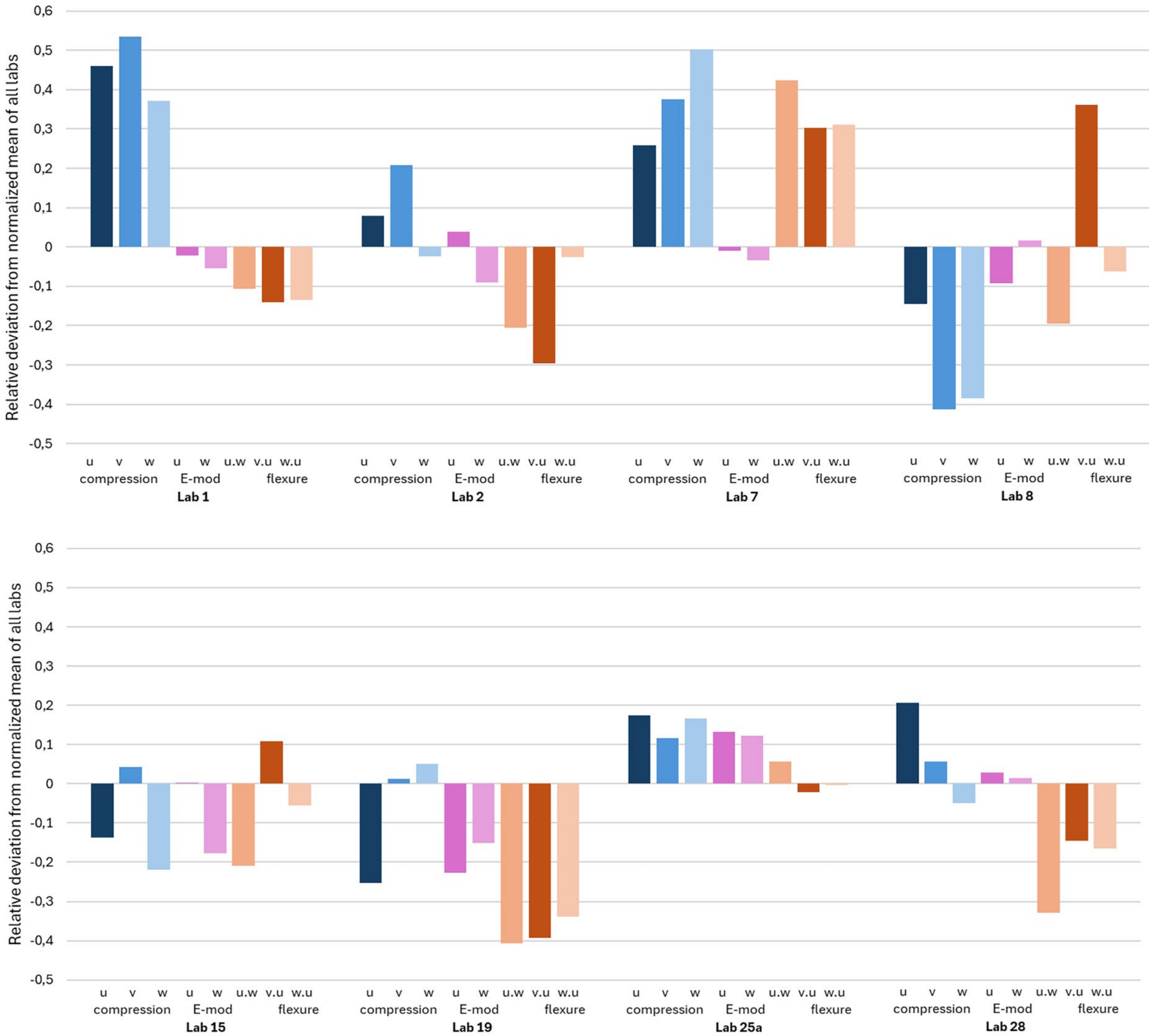

Fig. 20 Relative experimental properties (i.e. printed as a percentage of cast) from compression (3 orientations), E-modulus (2 orientations), and flexural (3 orientations) testing obtained from the 8 laboratories which performed all these tests, normalized to the average relative properties obtained from all laboratories minus 1. Thus, the 0 horizontal represents the normalized mean over all contributions. Example: if a property has a value of + 0.1, this indicates the ratio between cast and printed specimens was 10% higher than the overall mean ratio for all contributions; if the overall mean ratio was 80%, than it was 88% in this contribution

can actually be established, e.g. between test types or testing orientations, with a varying degree of significance. The reader is referred to these publications for more information. However, the practical implications of those findings, such as a potentially reduced need for testing different parameters, are not directly obvious, as it cannot (yet) be known whether an individual material-system combination produces outlier results, unless an extensive part of the experimental program has been performed. This will be subject of further consideration by the TC 304-ADC.

7 Feedback and experiences regarding instructions

Following the testing phase, we collected experiences and feedback from the different participating laboratories in order to analyze potential issues and evaluate the efficacy of the procedures herein proposed. Being a large testing campaign, different sources of issues were found but most of them were related to the preparation of specimens.

7.1 Specimen preparation

7.1.1 Printing path design and execution

The Study Plan requires all adjacent print paths to travel in the same direction. For concrete scale specimens that require relatively large print objects, this can require some extensive print path planning that can be challenging particularly when the available print bed is relatively small. This requirement was therefore not maintained by all laboratories. Instead, adjacent print paths were sometimes orientated back and forth.

7.1.2 Layer/specimen orientation

In a practical sense, it can be a challenge to correctly apply the orientation during testing. This requires specimens to be properly marked when extraction from the print object, because the layer structure and printing direction can usually not be identified with the naked eye after sawing or drilling. Following the marking instructions in the Study Plan is fundamental to ensure specimens are tested in the correct orientation and with the interfaces in the middle of a specimen. It is important to communicate the significance of this to laboratory staff, as this can easily be overlooked during specimen preparation, which can lead to contamination of the results. Outlining each individual interface (as required in the Study Plan), however, may be redundant and can be difficult and time consuming when a relatively small filament size is used. This may be further complicated by the fact that the top surface of a filament is actually not always flat, as typically assumed, but can demonstrate considerable curvature.

7.1.3 Sawing operations

The sawing of specimens from the print objects is labor intensive, particularly because according to the Study Plan each cube or beam specimen had 6 unique cutting surfaces. In the future, it may be considered to saw adjacent specimens, so that less saw cuts have to be made. This would also reduce waste. Furthermore, depending on the quality of the sawing equipment, it is generally difficult to obtain sawn specimens with parallel surfaces. This can be particularly challenging for the smaller mortar scale specimens. Capping or grinding, as specified by the Study Plan, is indeed needed for compression and E-modulus testing, to achieve parallel surfaces. Specific attention is needed when Digital Image Correlation (DIC) is used to measure strains rather than Linear Variable Differential transformers (LVDT) as this method is more sensitive to the alignment of surfaces.

The sawing process may also induce (visible) chipping as well microcracks in the surface that cannot be detected with the naked eye. In case of excessive chipping, specimens could be rejected, but a criterion for rejection has not yet been defined. The occurrence of microcracks, the extent of which would depend on the equipment and sawing process used, may contribute to an explanation regarding the variability in the results that have been obtained. Alternative to sawing, some laboratories also obtained specimens by core-drilling. Experience shows this may have considerable benefits. Specimens are easier and faster to cut, with higher accuracy and less need effort of (parallel) surface finishing. Possibly as a result, the standard deviation in compression and splitting tensile tests was lower than for sawn cube specimens. Disadvantages might be the unsuitability of the specimen geometry for flexural testing and a potentially higher waste of material, as less specimens can be obtained from the same print object volume.

7.1.4 Material usage

Because specimens are extracted from printed objects with considerable unusable areas, a high volume of material is needed to obtain a relatively limited number of specimens. This applies particularly to concrete scale testing. It may be reduced by optimizing the print object geometry, but the production of waste cannot be avoided entirely. Furthermore, the results may be less representative for practical applications, but further study is required to establish whether this is relevant.

7.2 Execution of tests

The recommended environmental conditions, particularly the relative humidity, was found to be hard to achieve in some laboratories. The mechanical tests themselves are relatively straightforward and posed few difficulties. However, not every test set-up is commonly available. The uniaxial test is known to be labor intensive. In the E-modulus test on mortar-scale, it can be difficult to place LVDTs on the beam specimens due to their small size. This is reflected by the relatively low response for this test (see Fig. 6).

7.3 Reporting

The reporting of mechanical properties data is a simple and long-established task that did not cause many difficulties. However, all aspects related to the printing process, including fresh material properties, print facility characteristics and print session data, and orientations in specimens, lack standardized reporting formats. This resulted in many mistakes and omissions in the submitted data. In more than half of the submitted contributions, corrections had to be made to ensure the analyses were performed based on correct data. Although most key data could thus be secured, more extensive analyses may have been possible when all optional parameters had been reported upon. This underlines the importance of establishing clear, standardized reporting parameters related to the print process.

In general reflection, the dispersion of results shown in Sect. 6 might indicate that the relevant parameters were not or not sufficiently recorded and that they have an unknown influence on the experimental results. It is suggested that a quality assessment scheme to categorize printing sessions and/or printed objects may help to determine the suitability of obtained specimens for mechanical characterization and therewith reduce the observed variability in results. However, it is yet unclear what the criteria for such an assessment should be. This requires the development of a theoretical framework.

8 Conclusion

This paper presented the approach and main results of a large interlaboratory study into the mechanical properties of 3D printed concrete. It outlined the objective, specimen preparation, and experimental procedure as well as the considerations that determined them. The study yielded 34 contributions from 30 laboratories in 19 countries. In total approximately 5,000 specimens were tested. Although two other associated papers analyze the results more in-depth, the main results with regard to compression, flexural bending and E-modulus were presented here.

Overall, the procedures presented in the Study Plan were found to be feasible and unambiguous, notwithstanding some minor improvements that can be made. The large number of results allows some broad conclusions regarding the state of development of 3D concrete printing and the mechanical properties obtained, beyond what can be concluded from smaller studies. The consistent experimental method that was maintained by the wide range of laboratories allowed setting up an open database that can be used not only for current but also for future analyses. This may contribute significantly to the development of codes for structural engineering and quality control of 3DCP. Furthermore, new data can be added later so that developments can be incorporated, which is highly important in a field that is still experiencing rapid development, both on the side of material and equipment design and integration. The TC 304-ADC intends to develop RILEM Recommendations to determine the mechanical properties of 3D printed concrete based on the Study Plan, the results of this study, and the evaluation of the applied experimental procedures, as presented in this and the associated papers and data sets [19–21, 23].

The initial analysis presented here, based on all validated submitted data, did not find fully consistent quantitative correlations between (i) the relative mechanical properties of cast and printed specimens, (ii) the relative mechanical properties of printed specimens tested under different orientations, (iii) the various relative mechanical properties tested, (iv) material characteristics and the relative mechanical properties, and (v) print facility characteristics and the relative mechanical properties. However, further data analysis presented in [21] and [22] shows that certain correlations can be established, e.g. between test types or testing orientations. This requires extensive identification and elimination procedures of outliers, to obtain significant results.

As significant variations on the level of individual contributions still occur, a single (or limited number of) parameter(s) cannot yet be identified to act as an appropriate measure of quality or overall indicator of mechanical properties; indeed, a wider experimental based approach is required to fully characterize the mechanical properties of printed materials. Furthermore, material properties cannot be determined independently of the printing system on which it is used.

A more extensive theoretical framework is needed to explain the observed variability in outcomes, possibly in relation to the interface presence in the print objects. It may be expected that, in addition to the material and process characteristics already queried in this study, more process data is needed to support the development and verification of such a framework.

Acknowledgements The authors wish to express their sincere gratitude to all those that have contributed to the RILEM TC 304-ADC ILS-mech interlaboratory study, in particular: Shravan Muthukrishnan (TUD Dresden University of Technology / Swinburne University of Technology), Jelle Versteege (Eindhoven University of Technology), Onur Ozturk, Nilufer Ozyurt Zihnioglu (Bogazici University), Josef Roupec (Brno University of Technology), Christiane Richter, Jörg Jungwirth (Munich University of Applied Sciences), Luiza Miranda (Ghent University), Rebecca Ammann (ETH Zurich), Jean-François Caron, Victor de Bono (Ecole des Ponts ParisTech), Renata Monte (University of São Paulo), Iván Navarrete, Claudia Eugenin (Pontificia Universidad Catolica de Chile), Maris Sinka, Alise Sapata (Riga Technical University), Ilhame Harbouz (Université de Sherbrooke), Jacques Kruger (Stellenbosch University), Jiří Vambera (ICE Industrial Services and Brno University of Technology), Mateja Štefančič, Katarina Šter, Aljoša Šajna, Lucija Hanžič (ZAG—Slovenian National Building and Civil Engineering Institute), Abdelhak Kaci (CY Cergy Paris Université), Passarin Jongvisuttisun (SCG Cement-building materials), Arun Arunothayan (Swinburne University of Technology), Zhao Zengfeng (Tongji University), Inka Mai, Inken Rasehorn, Dietmar Stephan (Technical University of Berlin), David Böhler, Niklas Freund, Dirk Lowke (Technical University of Braunschweig), Tobias Neef, Steffen Müller, Markus Taubert (TUD Dresden University of Technology), Daniel Auer, C. Maximilian Hechtl, Maximilian Dahlenburg (Technical University of Munich), Laura Esposito (Heidelberg Materials), Denisa Jancarikova (Czech Research Institute for Building Materials), Xingzi Liu (Loughborough University), Zhendi Wang (China Building Materials Academy), Kolluru Subramaniam (Indian Institute of Technology Hyderabad). Furthermore, the authors would like to acknowledge the input for Section 7 of this paper, received from Rebecca Ammann, Lucija Hanžič, Kolluru Subramaniam, Jacques Kruger, Xingzi Liu, Iván Navarrete, Māris Šinka, and Zengfeng Zhao.

Funding Open Access funding enabled and organized by Projekt DEAL.

Data availability The study plan for this interlaboratory study on mechanical properties of 3D printed concrete is publicly available as dataset [19] from mediaTUM at https://doi.org/10.14459/2023mp1705940. The processed and selected results used for the analyses presented in this paper have been published as dataset on Zenodo [23] at https://doi.org/10.5281/zenodo.12200570. This dataset is only available to participating laboratories until the embargo date 1.7.2025. After that, it will be publicly accessible.

Appendix A

List of the laboratories that have participated until the time of writing of this paper and whose results have been used in the analyses provided in this paper and the associated papers [21] and [22]. The list order is alphabetical and does not correspond to the laboratory numbering maintained in the papers.

- Bogazici University, Istanbul, Turkiye
- Brno University of Technology, Czech Republic
- Brno University of Technology in collaboration with ICE Industrial Services, Czech Republic
- Cergy Paris Université, France
- China Building Materials Academy, Beijing, China
- Ecole des Ponts ParisTech, France
- Eindhoven University of Technology, the Netherlands
- ETH Zürich, Switzerland
- Ghent University, Belgium
- Holcim Innovation Center, Lyon, France, in collaboration with Cobod International, Denmark
- Indian Institute of Technology Madras in collaboration with Tvasta Manufacturing Pvt. Ltd., India
- Indian Institute of Technology Hyderabad, India
- Loughborough University, United Kingdom
- Munich University of Applied Sciences, Germany
- Pontificia Universidad Catolica de Chile, Santiago, Chile
- Research Institute for Building Materials, Brno, Czech Republic
- Riga Technical University, Latvia

- SCG Cement-building materials, Thailand
- ZAG Slovenian National Building and Civil Engineering Institute, Ljubljana, Slovenia
- Southeast University, Nanjing, China
- Stellenbosch University, South Africa
- Swinburne University of Technology, Melbourne, Australia
- Technical University of Berlin, Germany
- Technical University of Braunschweig, Germany
- Technical University of Dresden, Germany
- Technical University of Munich, Germany
- Tongji University, Shanghai, China
- Université de Sherbrooke, Canada
- University of Naples Federico II, Italy in collaboration with Heidelberg Materials, Germany
- University of São Paulo, Brazil

Table 3 Mean relative values of printed specimens as a percentage [%] of the cast specimen values of the same experiment and orientation for the same laboratory

LAB	Experiment and orientation							
	Compression			Flexure			E-modulus	
	comp_U	comp_V	comp_W	flex_U.W	flex_V.U	flex_W.U	emod_U	emod_W
1	134.0	121.8	118.3	69.8	91.3	90.8	88.7	81.0
2	99.1	95.8	84.2	62.0	74.7	102.1	94.2	77.9
3	73.8	60.9	71.1	64.4	88.5	83.0	78.2	
4	64.3	68.0	68.8	105.4	142.4	139.6	101.2	89.6
5	111.6	64.1	99.9	81.8	117.1	109.9		
6					116.1	124.7		
7	115.5	109.1	129.6	111.2	138.3	137.4	89.8	82.6
8	78.5	46.6	53.0	62.8	144.6	98.3	82.4	87.1
9	53.9	72.4	67.2	33.0	85.2	93.2		
10		88.0	92.3	82.3	76.2	87.2		
11	86.3	71.4	57.6	78.1	105.9	115.9		
12	71.4	75.2	75.7	92.2	115.8	117.9		
13	90.5	88.2	79.7	72.7	99.1	96.8		
14	172.4	154.9	171.4	95.8	128.7	137.6		
15	79.3	82.6	67.4	61.7	117.8	98.9	90.8	70.5
16	80.4	80.3	69.7	119.7	211.1	201.1		
17	90.1	64.6	74.8	116.5	96.4	89.8		
18a	81.2	62.6	81.9	90.6	112.0	91.0		
18b	81.5	57.2	95.2	68.1	82.2	60.5		
19	68.5	80.3	90.7	46.4	64.4	69.3	70.1	72.7
20	94.9	72.6	93.2		111.9	114.2		
21	107.1	71.1	87.0					
22	77.0	83.3	86.0	81.6	91.3	108.0		
23	86.3	71.7	80.5	66.8	84.3	72.1		
25a	107.8	88.5	100.7	82.5	103.9	104.4	102.7	96.2
25b				110.3	106.1	121.5	93.3	86.6
25c				96.5	112.4	118.4	103.8	110.9
26	97.2	90.7	87.3	84.5	113.3	121.2		
27	82.0	64.4	69.5	17.5	44.5	36.4		
28	110.8	83.7	82.0	52.4	90.7	87.4	93.3	86.8
29	95.2	73.6	110.6					
30	79.4	56.0	57.1	81.3	120.3	115.1		
OVERALL MEAN	91.8	79.3	86.3	78.1	106.2	104.8	90.7	85.6

Appendix B

Table 3 presents the mean relative values of printed specimens as a percentage of the cast specimen values, organized by contribution, for each experiment and orientation presented in Figures 12, 13, 14, 15, 16, 17, 18 and 19. The mean of all contributions is also listed.

References

1. Bos FP, Menna C, Pradena M, Kreiger E, Leal da Silva WR, Rehman AU, Weger D, Wolfs RJM, Zhang Y, Ferrara L, Mechtcherine V (2022) The realities of additively manufactured concrete structures in practice. Cem Concr Res 156:106746. https://doi.org/10.1016/j.cemconres.2022.106746
2. Buchli J, Giftthaler M, Kumar N, Lussi M, Sandy T, Dörfler K, Hack N (2018) Digital in situ fabrication—Challenges and opportunities for robotic in situ fabrication in architecture, construction, and beyond. Cem Concr Res 112:66–75. https://doi.org/10.1016/j.cemconres.2018.05.013
3. Buswell RA, Leal da Silva WR, Bos FP, Schipper HR, Lowke D, Hack N, Kloft H, Mechtcherine V, Wangler T, Roussel N (2020) A process classification framework for defining and describing Digital Fabrication with Concrete. Cem Concr Res 134:106068. https://doi.org/10.1016/j.cemconres.2020.106068
4. Ma G, Buswell R, da Silva WRL, Wang L, Xu J, Jones SZ (2022) Technology readiness: A global snapshot of 3D concrete printing and the frontiers for development. Cem Concr Res 156:106774
5. Roussel N, Lowke D (eds) (2022) Digital Fabrication with Cement-Based Materials: State-of-the-Art Report of the RILEM TC 276-DFC. Springer International Publishing, Cham
6. Flatt RJ, Wangler T (2022) On sustainability and digital fabrication with concrete. Cem Concr Res 158:106837
7. Bischof P, Mata-Falcon J, Kaufmann W (2022) Fostering innovative and sustainable mass-market construction using digital fabrication with concrete. Cem Concr Res 161:106948
8. EN 1992–1–1:2004, EN 1992–1–2:2004, EN 1992–2:2005, EN 1992–3: 2006
9. ACI CODE-318–19(22): Building Code Requirements for Structural Concrete and Commentary (Reapproved 2022).
10. Fib Model Code for Concrete Structures (2020) ISBN 978–2–88394–175–5.
11. Tuvayanond W, Prasittisopin L (2023) Design for manufacture and assembly of digital fabrication and additive manufacturing in construction: a review. Buildings 13(2):429
12. Rubin AP, Quintanilha LC, Repette WL (2023) Influence of structuration rate, with hydration accelerating admixture, on the physical and mechanical properties of concrete for 3D printing. Constr Build Mater 363:129826
13. Mechtcherine V, Van Tittelboom K, Kazemian A, Kreiger E, Nematollahi B, Nerella VN, Bos F (2022) A roadmap for quality control of hardening and hardened printed concrete. Cem Concr Res 157:106800 https://doi.org/10.1016/j.cemconres.2022.106800
14. Bos F, Wolfs R, Theo Salet CCR, Concrete D (2020) SI: Editorial. Cem Concr Res. https://doi.org/10.1016/j.cemconres.2020.106157
15. Le T, Austin SA, Lim S, Buswell RA, Law R, Gibb AGF, Thorpe T (2012) Hardened properties of high-performance printing concrete. Cem Concr Res 42(3):558–566. https://doi.org/10.1016/j.cemconres.2011.12.003
16. Nerella VN, Hempel S, Mechtcherine V (2019) Effects of layer-interface properties on mechanical performance of concrete elements produced by extrusion-based 3D-printing. Constr Build Mater 205:586–601. https://doi.org/10.1016/j.conbuildmat.2019.01.235
17. Wolfs RJM, Bos FP, Salet TAM (2019) Hardened properties of 3D printed concrete: the influence of process parameters on interlayer adhesion. Cem Concr Res 119:132–140. https://doi.org/10.1016/j.cemconres.2019.02.017
18. ISO/ASTM 52939: (2023) Additive manufacturing for construction — Qualification principles — Structural and infrastructure elements
19. Bos F, Mechtcherine V, Roussel N, Menna C, Wolfs R, Lombois-Burger H, Baz B, Weger D, Moro S, Nematollahi B, Santhanam M, Zhang Y, Bhattacherjee S, Jia Z, Chen Y (2023) RILEM TC 304-ADC ILS-mech Study Plan, 13.04.2023. Published on MediaTUM. https://doi.org/10.14459/2023mp1705940.
20. Robens-Radermacher A, Kujath C, Bos F, Mechtcherine V, Unger JF (2025) Mechanical properties of 3D printed concrete: a RILEM TC 304-ADC Interlaboratory Study – Design and Implementation of a Database System for Querying, Sharing, and Analyzing Experimental Data. *Manuscript accepted for this Materials & Structures Topical Issue*. https://doi.org/10.1617/s11527-025-02650-9.
21. Mechtcherine V, Muthukrishnan S, Robens-Radermacher A, Wolfs R, Versteege J,Menna C, Ozturk O, Ozyurt N, Roupec J, Richter C, Jungwirth J, Miranda L, Ammann R,Caron JF, de Bono V, Monte R, Navarrete I, Eugenin C, Lombois-Burger H, Baz B, Sinka M,Sapata A, Harbouz I, Zhang Y, Jia Z, Kruger J, Mostert JP, Štefančič M, Hanžič L, Kaci A,Rahal S, Santhanam M, Bhattacherjee S,

Snguanyat C, Arunothayan A, Zhao Z, Mai I,Rasehorn IJ, Böhler D, Freund N, Lowke D, Neef T, Taubert M, Auer D, Hechtl CM,Dahlenburg M, Esposito L, Buswell R, Kolawole J, Isa MN, Liu X, Wang Z, Subramaniam K,Bos F (2025) Mechanical Properties of 3D Printed Concrete: a RILEM 304-ADCInterlaboratory Study – Compressive Strength and Modulus of Elasticity. *Manuscriptaccepted for this Materials & Structures Topical Issue*. https://doi.org/10.1617/s11527-025-02688-9.

22. Wolfs R, Versteege J, Santhanam M, Bhattacherjee S, Bos F, Robens-Radermacher A,Muthukrishnan S, Menna C, Ozturk O, Ozyurt N, Roupec J, Richter C, Jungwirth J, MirandaL, Ammann R, Caron JF, de Bono V, Monte R, Navarrete I, Eugenin C, Lombois-Burger H,Baz B, Sinka M, Sapata A, HarbouzI, Zhang Y, Jia Z, Kruger J, Mostert JP, Šter K, Šajna A,Kaci A, Rahal S, Snguanyat C, Arunothayan A, Zhao Z, Mai I, Rasehorn IJ, Böhler D, FreundN, Lowke D, Neef T, Taubert M, Auer D, Hechtl CM, Dahlenburg M, Esposito L, Buswell R,Kolawole J, Isa MN, Liu X, Wang Z, Subramaniam K, Mechtcherine V (2025) MechanicalProperties of 3D Printed Concrete: a RILEM TC 304-ADC Interlaboratory Study – Flexuraland Tensile Strength. *Manuscript accepted for this Materials & Structures Topical Issue*.https://doi.org/10.1617/s11527-025-02687-w.
23. Bos F, Robens-Radermacher A, Muthukrishnan S, Versteege J, Wolfs R, Santhanam M, Menna C, Mechtcherine V (2024) Database of the RILEM TC 304-ADC interlaboratory study on mechanical properties of 3D printed concrete (ILS-mech). 2024. https://doi.org/10.5281/zenodo.12200570. Embargoed until 1 July 2025.
24. Neville A (2012) Properties of Concrete 5th edition (Harlow. 2012, Pearson Education), Chapter 12 Testing of hardened concrete, ISBN: 978–0–273–75580–7
25. EN 196–1: (2016) Methods of testing cement Determination of strength
26. EN 12390–13 (2013) Testing hardened concrete–Part 13: determination of secant modulus of elasticity in compression. British Standards Institution: London, UK, 2013